PCCP

Cite this: *Phys. Chem. Chem. Phys.*, 2011, **13**, 15384–15402

www.rsc.org/pccp

PERSPECTIVE

Graphene-based electrochemical energy conversion and storage: fuel cells, supercapacitors and lithium ion batteries

Junbo Hou,*[a] Yuyan Shao,[b] Michael W. Ellis,[c] Robert B. Moore[d] and Baolian Yi[e]

Received 7th March 2011, Accepted 1st July 2011
DOI: 10.1039/c1cp21915d

Graphene has attracted extensive research interest due to its strictly 2-dimensional (2D) structure, which results in its unique electronic, thermal, mechanical, and chemical properties and potential technical applications. These remarkable characteristics of graphene, along with the inherent benefits of a carbon material, make it a promising candidate for application in electrochemical energy devices. This article reviews the methods of graphene preparation, introduces the unique electrochemical behavior of graphene, and summarizes the recent research and development on graphene-based fuel cells, supercapacitors and lithium ion batteries. In addition, promising areas are identified for the future development of graphene-based materials in electrochemical energy conversion and storage systems.

1. Introduction

Today, global energy use is growing dramatically due to steadily rising energy demand in developed nations and rapidly increasing demand in the emerging economies. Meeting this growing energy demand while avoiding resource depletion and long-term damage to the environment requires the development of high performance, low cost and environmentally benign energy systems. Improved technologies for the production and storage of electrical energy are crucial to improving the way that society uses energy. Therefore, large-scale research efforts are underway in various locations around the world to develop fuel cells for the direct production of electricity from chemical energy and to develop supercapacitors and advanced batteries for electrical storage. These new technologies are particularly important to mobile and automotive applications. The realization of high performance energy conversion and storage devices will likely require the development of novel materials. Carbon materials have attracted considerable interest in electrochemical applications due to their abundance, processibility, stability, and relatively environmentally friendly

[a] *Institute for Critical Technology and Applied Science, Virginia Tech, Blacksburg, Virginia 24061, USA. E-mail: junbo80@vt.edu, junbo.hou@yahoo.com*
[b] *Pacific Northwest National Laboratory, Richland, WA 99352, USA*
[c] *Department of Mechanical Engineering, Virginia Tech, Blacksburg, Virginia 24061, USA*
[d] *Department of Chemistry, Virginia Tech, Blacksburg, Virginia 24061, USA*
[e] *Dalian Institute of Chemical Physics, Chinese Academy of Sciences, Dalian, 116023, China*

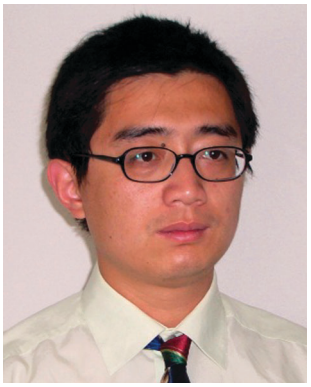

Junbo Hou

Junbo Hou is currently a Research Associate in Institute for Critical Technology and Applied Science at Virginia Tech. He received his PhD degree (2008) in Chemical Engineering from Dalian Institute of Chemical Physics, Chinese Academy of Sciences, studying on fuel cell technologies and electrochemical fundamentals. After working on semiconducting materials synthesis and characterization for two years in University of Leoben and Erich Schmid Institute, Austria Academy of Science, he came to Virginia Tech and works on the electrochemical energy conversion and storage.

Yuyan Shao

Yuyan Shao is currently a Senior Scientist in the Chemical & Materials Sciences Division at the U.S. DOE Pacific Northwest National Laboratory (PNNL). Dr Shao received his PhD at Harbin Institute of Technology in 2006. He did his post-doctoral research at Case Western Reserve University and PNNL. His research interest is focused on electrochemical energy storage and conversion. He is active in fundamental study and high-performance materials for fuel cells, batteries, supercapacitors, etc.

characteristics. In particular, chemical stability across a wide temperature range in either acidic or basic solution makes carbon materials extremely attractive for use as electrodes in electrochemical energy devices.

Graphene, a form of carbon experimentally demonstrated in 2004,[1] consists of a monolayer of carbon atoms sp^2 bonded into a two dimensional sheet. Graphene is a basic building block for graphitic materials of all other dimensionalities as illustrated in Fig. 1.[2] Graphene possesses unique electronic properties, including: ambipolar electric field effect, extremely high mobility of charge carriers (up to 10^5 cm^2 V^{-1} s^{-1}), mass-less electron, quantum Hall effects (QHE) even at room temperature, and electron wave propagation within a one atom thick layer.[2,3] The unique properties of graphene have sparked widespread interest and investigations in laboratories around the world. But despite the surge in interest, the chemical and physical understanding of graphene is still evolving as are the potential applications.

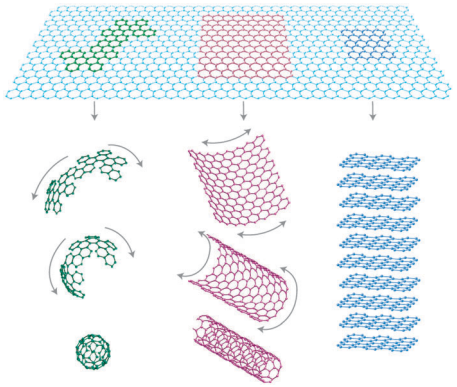

Fig. 1 Graphitic family: 0-dimensional fullerene, 1-dimensional carbon nanotube, 2-dimensional graphene, 3-dimensional graphite.[2]

Unquestionably, graphene provides a wealth of opportunities for study in the fields of chemistry, materials science, and physics. In addition, there are also considerable opportunities for advances based on graphene mechanical and thermal properties. For example, graphene shows very high intrinsic strength (~130 GPa) and Young's modulus (~1.0 TPa), making it the strongest material ever measured.[4] Further, it can be stretched to deformations well beyond the linear regime.[4] The thermal conductivity of graphene at room temperature can reach $\sim 5 \times 10^3$ W m^{-1} K^{-1} (for comparison, copper is 400 W m^{-1} K^{-1}) which suggests potential uses for thermal management in a variety of applications including electronics.[5] Graphene shows very high surface area (~2600 m^2 g^{-1}), much larger than the surface areas of graphite (~10 m^2 g^{-1}) and carbon nanotubes (1300 m^2 g^{-1}).[6] These remarkable properties make graphene promising in applications such as polymer-composite materials,[6,7] paper-like materials,[8] photo-electronics,[9–11] field effect transistors,[12] electro-mechanical systems,[13,14] sensors and probes,[15–17] hydrogen storage,[18] and of course electrochemical energy systems.[19]

Michael W. Ellis

Michael W. Ellis is an Associate Professor of Mechanical Engineering at Virginia Tech. Dr Ellis has 25 years of experience in engineering, research, and education related to advanced energy systems. His current work focuses on the development and evaluation of materials for PEM fuel cell membranes and diffusion media, modeling liquid transport in PEM fuel cells, and fuel cell cogeneration for buildings. He teaches courses in thermodynamics, sustainable energy, and engineering design. Dr Ellis is the director of the Sustainable Energy Research Program in Virginia Tech's Institute for Critical Technology and Applied Science and is chair of ASME's Advanced Energy Systems Division.

Robert B. Moore

Robert B. Moore is the Associate Director for Research at the Virginia Tech Institute for Critical Technology and Applied Science (ICTAS), and a Full Professor in the Department of Chemistry at Virginia Tech, with 22 years of academic experience in the field of Polymer Physical Chemistry. His research is focused in the area of ion-containing polymers for energy applications, with specific interests that include: control of morphology-transport property relationships in proton exchange membrane fuel cell systems, tailored actuation behavior in nano-structured materials, and the use of small-angle X-ray and neutron scattering methods for the characterization of morphology in ion-containing polymers.

Baolian Yi

Baolian Yi is a fellow of the Chinese Academy of Engineering, and a Professor of Chemical Engineering at Dalian Institute of Chemical Physics, Chinese Academy of Sciences. He has been working on the research and development of fuel cells and related fields since 1970's. He researched on AFC for space application in 1970's, and conducted fuel cell technique to aqueous solution electrolysis industry and electrochemical sensors in 1980's. During 1990's, He initiated the researches on PEMFC, MCFC and SOFC. He has authored more than 150 Journal papers and 50 patents.

In this paper, we focus on the electrochemical applications of graphene which are derived from its properties such as high specific surface area, high conductivity and chemical stability. We review the rapidly growing body of knowledge in this field, organizing the review into a discussion of the preparation of graphene and a discussion of its application in electrochemical energy conversion and storage devices including fuel cells, supercapacitors and lithium ion batteries.

2. Preparation of graphene

Mechanical exfoliation

In 2004, graphene was demonstrated by mechanically separating individual graphene sheets from a strongly bonded layered structure such as graphite.[1,20] This technique yields graphene samples that are virtually free of crystal defects and that consequently have carrier mobilities up to 2×10^5 cm^2 V^{-1} s^{-1}.[21] It is very difficult to scale this process to mass production. Another kind of mechanical exfoliation method is based on the concept of anodic bonding. In this approach, bulk graphite was bonded onto borosilicate glass under a particular temperature and voltage and then peeled away leaving behind a single-layer or few-layer sheet of graphene on the substrate.[22]

Ultrasonic cleavage

In a conceptually similar method, referred to as ultrasonic cleavage, graphene precursors are suspended in water or organic solvents, and then ultrasonic agitation is used to supply the energy to cleave the graphene precursors.[23,24] This idea is based on the experimental observation that CNTs can be successfully exfoliated in solvents such as N-methylpyrrolidone (NMP).[25] The success of ultrasonic cleavage depends on the proper choice of solvents and surfactants as well as the sonication frequency, amplitude and time.[26,27]

Epitaxial growth on SiC

The success of techniques employed for silicon-based microelectronics have inspired the investigation of these techniques for the fabrication and processing of graphene materials. With this approach, graphene is produced on the Si-terminated face of single-crystal H-SiC by thermal desorption of Si, which leaves behind a 2–3 layer thick graphene sheet.[28–30] Unfortunately, this method is not adapted to prepare one atom thick graphene. Also, achieving large graphene domains with uniform thickness remains a challenge. Because SiC automatically supplies an insulating substrate, this method actually provides a direct route to the preparation of a SiC supported graphene wafer which can then be nanopatterned for electronic applications using conventional lithography methods.[28]

Chemical vapor deposition

Graphene sheets can also be prepared on metallic surfaces. Graphene monolayers with high structural quality were obtained by low-pressure chemical vapor deposition (CVD) of ethylene on a hot Ir (111) surface.[31] With this process, free-standing graphene films cannot be obtained nor can films be transferred to other substrates as Ir is extremely difficult to etch. Another example of the formation of graphene films from the decomposition of vapor deposited hydrocarbons is the epitaxial growth on Ru (0001) to produce arrays of macroscopic single-crystalline graphene domains in a controlled, layer-by-layer fashion.[32] In addition to growth on single-crystalline metals, large-scale graphene films can also be directly synthesized by CVD on poly-crystalline nickel substrates.[9] Later this method was improved to operate under ambient pressure. The resulting graphene films (1–12 graphene layers) can be ascribed to C segregation on the Ni surface following deposition from the bulk.[10] In contrast to Ni substrates, the growth of large-area (centimeter-scale) graphene films by CVD using methane (at 1000 °C) can be facilitated on copper substrates since carbon has a low solubility in Cu and since annealed Cu can exhibit very large grains.[12,33] Another method is the reaction of carbon monoxide (CO) with aluminum sulfide (Al_2S_3).[34] The precise mechanism of the graphene growth on the poly-crystalline metals is still not clear. But, the solubility and segregation behavior are definitely different at grains and grain boundaries in the poly-crystalline metals. Graphene nuclei morphology and carbon diffusion are most likely not the same at grains and grain boundaries. In addition, non-planar surfaces caused by the annealing effect at high temperature make it difficult for the resulting graphene to bridge these gaps.

Unrolling CNT

Graphene sheets can be generated by unrolling CNTs.[35–37] In this process, NH_3-solvated Li^+ is electrostatically attracted into the negatively charged multi-layer CNTs (MWCNTs). The simultaneous intercalation of Li and NH_3 into MWCNTs can increase interlayer distances from 3.35 Å to 6.62 Å, allowing exfoliation and unwrapping (Fig. 2).[35] Another variation of the unrolling technique uses strong oxidizing agents $KMnO_4$ to cut along the longitudinal direction of MWCNTs.[36] This exfoliation process can be executed at room temperature. The use of an oxidizing agent can be avoided by using an Ar plasma etching method to unzip MWCNTs to produce graphene nanoribbons (GNRs).[38]

Thermal reduction

To produce graphene sheets by thermal expansion requires sufficient oxidation of graphite during the acid treatment and adequate pressure during the thermal heat treatment. When the decomposition rate of the epoxide and hydroxyl sites exceeds the diffusion rate of the evolved gases, pressure between the layers rises. If the interlayer pressure exceeds the van der Waals forces connecting the layers, the graphite oxide (a compound consisting of carbon, oxygen, and hydrogen

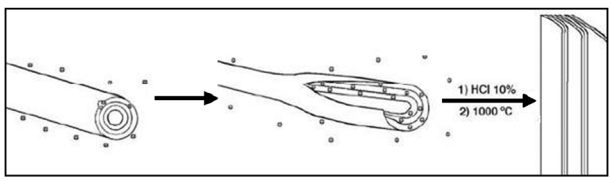

Fig. 2 Simultaneous intercalation of Li and NH_3 into MWNTs increases interlayer distance allowing exfoliation and unwrapping to form graphene nanoribbons.[35]

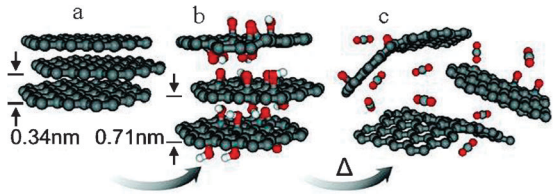

Fig. 3 Graphene is generated under thermal reduction: a graphite; b strong oxidization of graphite leads to formation of oxygen containing functional groups within the interlayer and thus increases interlayer distance; c exfoliation takes place once the rate of decomposition of the functional group is higher than that of the gas diffusion.[40]

maintains layered structure of graphite with much larger spacing) splits into individual sheets (Fig. 3).[39] A more detailed understanding of the mechanism of thermal exfoliation is presented in ref. 40. More recently, the process of thermal reduction has been modified by the use of microwave technology.[41] In this process, the first step is the pre-exfoliation of graphite by microwave heating.[42] Graphene oxide (a monomolecular-layer sheet consisting of carbon, oxygen, and hydrogen) is then dispersed in DMAc and water and thermally reduced using microwave treatment.[43] Another approach to thermal exfoliation involves heating a mixture of sodium and ethanol in a sealed reactor vessel at 220 °C for 72 h to yield a solvothermal product.[44] Recently, thermal exfoliated GNRs with narrow width (<10 nm) and smooth edges were prepared for use in room temperature transistor operations with excellent switching speed and high carrier mobility.[45]

Chemical reduction

In addition to the thermal reduction method, chemical reduction is another important method for preparing graphene.[46–48] The chemical reduction method involves complete exfoliation of graphite oxide into individual graphene oxide sheets followed by the *in situ* reduction of these graphene oxide sheets to produce individual graphene-like sheets. Fig. 4 schematically shows this method.[49] The graphite oxide is typically produced by the Hummers method.[50] Successful reduction of the exfoliated graphene oxide requires careful selection of the reducing agent, solvent, and/or surfactant to maintain a stable suspension. The reducing agent hydrazine hydrate is found to be the best one in producing very thin graphene-like sheets.[8,51] In addition to the hydrophilicity,[51] the surface charge of as-prepared graphene oxide sheets plays an important role in the suspension.[49] Two steps of reduction and sulfonation of the graphene oxide can increase the concentration of produced graphene to a reasonable value (2 mg mL^{-1}).[52] Further, the ammonia can be replaced by strong alkaline materials

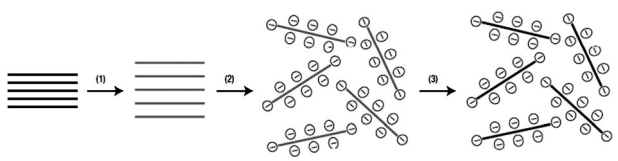

Fig. 4 Chemical reduction routine: (1) graphite is oxidized to graphite oxide; (2) exfoliation of graphite oxide yields graphene oxide suspended in solution; (3) chemical reduction of graphene oxide yields the conducting graphene.[49]

(*e.g.*, NaOH), greatly reducing the zeta potential of the aqueous suspension and leading to an enhanced surface charge on the graphene oxide.[53] To overcome the hydrophilicity and the electro-statistic effect, a surfactant can be used to encourage a stable suspension of graphene oxide.[54,55] A new approach for the fabrication of graphene sheets by ethylenediamine (EDA) reduction in DMF was reported.[56] Recently, the reducing agent trioctylphosphine (TOP) was applied to act as both a reducing agent and an aggregation-prevention surfactant.[57]

Doping

To tailor the semiconducting properties, chemical doping with N, B or small molecules can make *p*-type and *n*-type graphene. The introduction of *n*-type electronic doping can be accomplished by high temperature annealing (1100 °C) in NH_3.[58] Small molecules can be used for chemical doping, and poly(ethylene imine) and diazonium salts have been investigated as stable, complementary dopants on graphene.[59] Also, a new form of 2D atomic film consisting of hybridized h-BN and C (graphene) domains has been synthesized.[60] In addition to modification of the graphene layer itself, the doping can be performed *between* graphene layers. Graphene films up to eight layers have been effectively *p*-doped with nitric acid.[61] To increase the through-plane conductance, $AuCl_3$ solution can be put into graphene films.[11]

The production of large-area (*i.e.* cm^2) graphene at large scale should generally aim for low defect density, low cost and environmentally friendly processing. Based on a review of the current literature, it appears that most graphene based materials used in electrochemical devices are prepared using thermal reduction and chemical reduction. However, the research on the production of graphene sheets or nanoribbons is expanding rapidly, and new methods are emerging including bottom-up,[62] hydrogen arc discharge,[63] porphyrin exfoliation,[64] micromolding in capillary method,[65] wet ball milling[66] and electrochemical modification.[67] In addition, while the most appropriate preparation technique depends on the application,[68] a further consideration is that the edge structures and chemical terminations of graphene synthesized by various methods are often unknown and uncontrolled.

3. Graphene based electrochemical energy devices

The electrochemistry of graphene has been systematically investigated with respect to surface chemistry and structure, heterogeneous charge transfer rate constants on redox species, electrochemical operating window, and electrocatalysis of molecules.[69,70] The most notable feature of graphene is the very large electrochemically active surface area. Cyclic voltammetry shows a 13 times higher capacitance on graphene electrode than that on the bare glassy carbon (GC).[69] Calculated from chronocoulometric curves at different electrodes for the reduction of 1 mM $K_3Fe(CN)_6$ with 2 M KCl, the area for different electrodes is graphene/GC (0.092 cm^2) > GC electrodes (0.0706 cm^2) > graphite/GC (0.0560 cm^2).[70] Besides the very large physical surface area, the sp^2-hybridized structure may contribute to the high capacitance value particularly for graphene. Finally, as with other carbon

allotropes,[71] there are significant edge-plane-like defective sites existing on the surface of graphene.

Several systems including $Ru(NH_3)_6^{3+/2+}$, $Fe(CN)_6^{3-/4-}$, $Fe^{3+/2+}$, and dopamine (DA) have been used for testing the electrochemistry of graphene because of their well-known sensitivity and selectivity to the electronic properties, surface microstructure, and surface chemistry of carbon electrodes.[69,71] Voltammograms of these redox systems demonstrate fast charge transfer kinetics on a graphene electrode. Electrochemical impedance spectroscopy (EIS) shows that the graphene electrode possesses smaller charge transfer resistance compared with the graphite/GC and GC electrodes. In addition to its favorable surface characteristics, the electrochemical operating window for a graphene electrode in 0.1 M pH 7.0 PBS is 2.5 V, which is comparable to that for graphite and GC electrodes.[70] Finally, graphene prepared from graphite generally does not contain any heterogeneous impurities which is a significant advantage over CNTs.[72] The following sections discuss the implications of these and other graphene characteristics for electrochemical device applications including fuel cells, supercapacitors, and batteries.

3.1 Fuel cells

Polymer electrolyte membrane (PEM) fuel cells are electrochemical energy conversion devices, which have attracted considerable interest as power sources for mobile and stationary applications, with active research and development programs all over the world focused on this field in recent decades.[73,74] However, in spite of this effort, the cost and durability issues related to the materials and components still hinder the commercialization of PEM fuel cells. Graphene sheets, with their unique nanostructure and properties, are promising alternatives for several of the critical PEM fuel cell materials. As a carbon allotrope, the most obvious use for graphene is as a catalyst support. Generally, the catalyst support materials should have particular properties such as: (i) high specific surface area, improving the dispersion of catalytic metals, (ii) chemical stablility under oxidative and reductive conditions at relevant temperatures (150 °C or less for PEM fuel cells), (iii) high electrochemical stability under fuel cell operating conditions, (iv) high conductivity, and (v) easy recovery of Pt in the used catalyst.[75]

For porous electrodes, such as those employed in PEM fuel cells, the specific surface area of the catalyst support is a critical factor. For graphene, the theoretical specific surface area of graphene is about 2600 $m^2\ g^{-1}$, but the specific area of multilayer graphene decreases. The limiting case is graphite, having a specific surface area of only 10 $m^2\ g^{-1}$. If the graphene supported catalysts are prepared in one step, the chemical reductions of graphene oxide and the metal salts occur simultaneously. With this process, there are most likely single-, double-, and a few-layer graphene sheets as well as thin graphite films co-existing in the resulting supported catalyst. Thus, the actual specific surface area of the supported catalysts will be far below the theoretical value. Even so, the produced catalysts exhibit high electrocatalytic activity.[76–78]

In addition to the active surface area, the durability of the catalyst and the support is an important issue in fuel cell applications. There are two ways by which catalyst surface area is lost. One is coalescence sintering in which two catalyst clusters touch, and then fuse into one larger cluster. The other is Ostwald ripening in which atoms evaporated from one cluster transfer to another, creating one larger cluster.[75] Coalescence sintering is enhanced by carbon corrosion which occurs under high potential and acid environment (*i.e.*, the PEM fuel cell condition). In this process, the carbon support is oxidized into CO_2 or CO causing the catalyst support to collapse and thus causing coalescence sintering. In addition, when the carbon support is oxidized into surface oxygen-containing species, catalyst–carbon interactions will be weakened also facilitating coalescence sintering. Graphene may improve catalyst durability by providing a more stable support material and by strengthening the interaction of the catalyst with the support.

Finally, a high performance PEM fuel cell electrode requires the formation of numerous triple-phase boundaries (TPBs) to create efficient reaction sites at nanoscale or microscale. The TPB is accessible for mass transfer (reactants and products), protons, and electrons, and provides a site where electrochemical reactions can occur. The microstructure of the typical catalyst layer in the PEM fuel cells can be depicted as catalyzed carbon particles flooded with the electrolyte to form agglomerates covered with a thin film of electrolyte. The reactant gas first passes through the channels between the agglomerates, diffuses through the ionomer thin film and thereafter in the agglomerates, and then reaches the TPBs.[79] There are two main pore structures: the primary pores in the agglomerates with characteristic lengths on the order of nanometers or tens of nanometers; and the secondary pores between agglomerates with characteristic lengths from nanometer to micrometer. These pore structures are essential for gas and water transport. The unique planar geometry of graphene, coupled with its high electrical conductivity provides an opportunity to create particularly promising TPB architectures.

Research efforts to take advantage of the unique features of graphene to produce supported catalysts with enhanced activity, increased durability, and high performance electrode architectures are discussed in the following sections.

3.1.1 Enhanced electrocatalytic activity. The prospect for enhanced fuel cell catalysts through the use of a high specific surface area graphene support was explored by preparing graphene–metal particle nanocomposites.[76] This work demonstrated that graphene oxide can be reduced by ethylene glycol (EG), and thus, graphene–metal particle nanocomposites can be prepared in one step in the water-EG system using graphene oxide as a precursor with metal nanoparticles (Au, Pt and Pd). This approach has the additional advantage that the metal nanoparticles can be adsorbed on graphene oxide sheets and thus facilitates the catalytic reduction of graphene oxide with EG. The cyclic voltammogram of methanol oxidation on the prepared graphene–Pt nanocomposites demonstrates the potential application in direct methanol fuel cells. In a subsequent work, using the reducing agent $NaBH_4$, composites of graphene nanosheets decorated by Pt nanoclusters were prepared via reduction of graphite oxide and

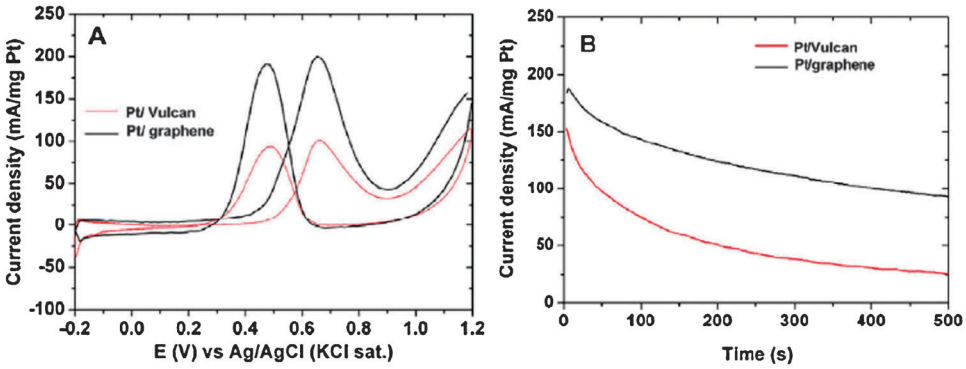

Fig. 5 Enhanced electrochemical activity toward methanol: (a) CV for Pt/graphene and Pt/Vulcan in nitrogen saturated aqueous solution of 0.5 M H_2SO_4 containing 0.5 M CH_3OH at a scan rate of 50 mV s^{-1}; (b) Chronoamperometric curves for the catalysts in the same solution at 0.6 V *vs.* Ag/AgCl.[77]

H_2PtCl_6 in one pot.[77] The electrochemically active surface area (ECSA) of the graphene-based catalyst is 44.6 m^2 g^{-1} while that of Pt/Vulcan is 30.1 m^2 g^{-1}, and further, the graphene-based catalyst shows superior catalytic performance toward methanol oxidation (Fig. 5).[77] An alternative synthesis approach, the rapid microwave method, was also used to produce a reduced graphene-oxide supported Pt.[78] It is also found that the increased hydroxyl species on the catalysts makes it CO resistant. Besides the direct methanol or ethanol fuel cells, graphene supported platinum also shows the higher electrocatalytic activity toward oxygen reduction.[80]

In addition to work with single-metal catalysts, bimetallic Pt–Ru nanoparticles have been synthesized on graphene sheets using the EG reduction method[81] and impregnation method.[82] Results showed that graphene-supported Pt and Pt–Ru nanoparticles demonstrate enhanced performance over the widely-used Vulcan XC-72R carbon black supported catalyst for both methanol and ethanol electro-oxidations with regard to diffusion efficiency, oxidation potential, forward oxidation peak current density, and the ratio of the forward peak current density to the reverse peak current density.[81] Using the metal precursors ($PtCl_2$ and $RuCl_3$) and the solvent tetrahydrofuran (THF), a Pt–Ru catalyst with a high metal content of 80 wt% was synthesized on the graphene sheets and showed superior electrochemical activity toward methanol oxidation compared with Pt–Ru/Vulcan XC-72R.[82] The enhanced catalytic activity was attributed to the higher utilization and activation of Pt or Pt–Ru on graphene sheets because of the higher specific surface area of graphene sheets which leads to a higher dispersion and better accessibility of Pt nanoparticles. From the preceding results, it appears that the higher electrochemical performance of graphene-supported catalysts is associated with the use of single-layer (high specific surface area) graphene sheets in the production of the catalyst. Confirmation that the superior electrocatalytic activity arises from the large surface area could be established by systematic studies of Pt nanoparticles dispersed on graphene sheets with tailored specific surface areas.

The enhanced electrocatalytic activity of graphene-supported catalysts may also be attributable to the graphene microstructure such as the functional groups and defects as well as to the interaction of Pt clusters with graphene. This hypothesis is supported by work which shows that functionalized graphene-supported Pt shows a higher electrochemical surface area and oxygen reduction activity as compared with commercial catalysts.[83] It was suggested that the graphene surface groups such as epoxy might function as anchoring sites for Pt precursor to prevent the aggregation of the Pt nanoparticles. This effect could contribute to improved dispersion of Pt nanoparticles on graphene sheets thus giving rise to the enhanced catalytic properties of the Pt cluster.[83]

Another interesting finding, demonstrated through scanning transmission electron microscopy (STEM) studies, is that Pt particles below 0.5 nm in size are formed on graphene sheets as illustrated in Fig. 6.[84] The small Pt particles were confirmed by high angle annular dark field (HAADF) image and energy dispersive X-ray spectroscopy (EDS). This graphene supported Pt was synthesized from the platinum precursor $Pt(NO_2)_2{\cdot}(NH_3)_2$ and from chemically reduced graphene using the impregnation method (Ar/H_2 at 400 °C). The resulting graphene-supported catalyst reveals an unusually high activity for methanol oxidation reaction compared to Pt/carbon black catalyst.[84] The author ascribed this enhanced electrocatalytic activity to the formation of dramatically smaller Pt particles. It is speculated that the strong interaction between Pt and graphene is responsible for the small Pt particles and thus might cause modulation in the electronic structure of the Pt clusters.

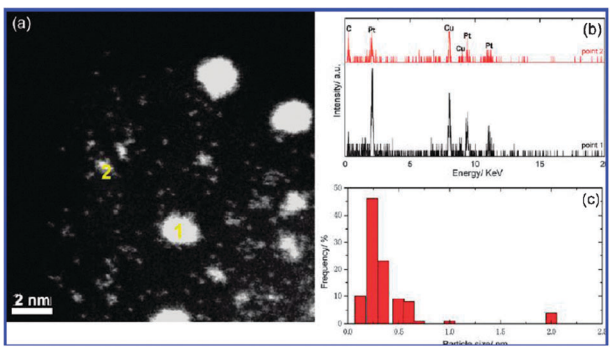

Fig. 6 Pt particles on the graphene sheets under STEM and Pt particles below 0.5 nm in size are observed: (a) HAADF image; (b) EDS spectrum; (c) Pt particle distribution.[84]

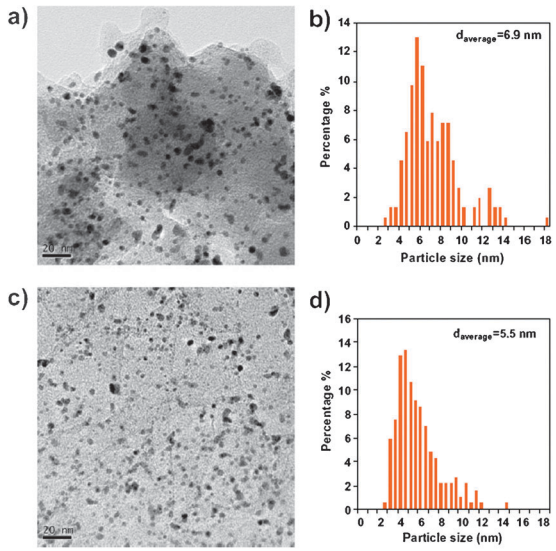

Fig. 7 TEM images of (a) E-TEK and (c) Pt-Graphene after 5000 CV degradation, and Pt nanoparticle size distribution diagrams on (b) E-TEK and (d) Pt-Graphene after 5000 CV degradation.[83]

Unlike carbon supports (*e.g.* activated carbons), graphene cannot exhibit micro-pores and deep cracks where deposited Pt nanoparticles would be isolated from the ionomer phase and thus unable to form electrochemically active TPBs. But carbon vacancies may exist in the produced graphene, especially in the chemically reduced graphene, where more charge, dangling bond and functional groups can be entrapped. These features could lead to different localized electronic structures in the graphene sheets and to interactions with catalyst precursors or metal clusters, and therefore may impact the electrocatalytic activity. Interestingly, the relation of the peak current density and the scan rate in the cyclic voltammograms indicates that methanol diffuses faster on the surfaces of graphene sheets than that on the carbon black and graphite substrate.[81]

Some of the preceding experimental studies are supported by theoretical studies showing that Pt bonds more strongly to functionalized graphene surfaces. From density functional theory (DFT) calculations, the gap between the highest occupied and lowest unoccupied molecular orbitals (the HOMO–LUMO gap) of hydrogen terminated graphene is smaller than the zero-gap in infinite-size graphene. The small HOMO–LUMO gap is still retained after a Pt cluster binds to an edge of a sp^2 C surface to form two Pt–C bonds.[85] This theoretical calculation demonstrates that Pt clusters bond more strongly to the surface of the hydrogen terminated graphene than to infinite-size graphene and that Pt clusters prefer the edge over the surface in the hydrogen terminated graphene. In addition, oxygen containing functional groups will not only function as anchoring sites for Pt precursors but also influence the position of Pt cluster on the graphene sheets and the bonding energy with the sp^2 carbon in the graphene.

Further research is needed to understand the mechanism by which electrocatalytic activity is enhanced on the graphene support. Specifically, studies comparing the performance of catalysts supported on defect-free and defect-rich graphene could help to explain the role of defects in electrocatalytic activity. Likewise, systematic control of surface functional groups or of electronic structure (using nitrogen-or boron-doping) could yield a deeper understanding of the relative influence of these features and suggest areas for further improvement of graphene supported catalysts.

3.1.2 Enhanced durability. The unique structure of graphene may improve electrode durability by strengthening the interaction between the catalyst particles and the graphene support. Using the accelerated degradation test (ADT) methods (potential step 1.4 V for 10 s to 0.85 V for 5 s), a poly(diallyldimethylammonium chloride) (PDDA) modified-graphene-supported Pt was compared to Pt/CNT and ETEK Pt/C.[86] After 46 h of testing, Pt/CNT and ETEK Pt/C degraded by 75% based on both ECSA and oxygen reduction reaction (ORR), but graphene supported Pt only degraded only 40% (ECSA) and 20% (ORR). In this test, the Pt morphology did not change, and the improved durability can be attributed to a more stable graphene support. In another durability test, Pt morphology did change and the influence of the support on the morphological stability was investigated.[83] After 5000 cycles of 0.6 to 1.1 V ADT, the average Pt particle size in a graphene-supported catalyst increased from 2 to 5.5 nm and more than 75% of the Pt particles remained smaller than 6.9 nm. For E-TEK carbon-supported catalysts, the average particle increased from 2.8 to 6.9 nm, and more than 45% of the particles were over 6.9 nm (Fig. 7). This result indicates that the interaction of Pt with graphene is stronger than the interaction with the E-TEK carbon support, thus leading to less Pt sintering on graphene than on ETEK carbon. The different observations between this study and the former study regarding Pt morphology changes may be attributable to the use of the reduction preparation method in the former study and of the impregnation-heat treatment method in the latter study. In another words, the use of H_2 and high temperature also changes structure of graphene sheets, creating H terminated graphene, and thus enhancing the Pt-sp^2 carbon bonding. As calculated by DFT, H terminated graphene has the advantage of enhancing the interactions between a Pt_6 cluster and an sp^2 carbon surface.[85]

As noted previously, nitrogen and boron can also be used to modify the electronic structure of the carbon support materials, thus improving the electrocatalytic activity and catalyst durability. The binding energy between a single platinum atom and several nitrogen-doped carbon graphene structures was evaluated using DFT.[87] The nitrogen doping can double the binding energy, with the increase in binding energy proportional to the number and proximity of nitrogen atoms to the carbon-platinum bond. It should be noted that the addition of N atoms increases the number of dislocations in the lattice because N is prone to form pentagonal defects in the graphene structure.[87]

3.1.3 Graphene based electrodes. The use of 2-D graphene as the catalyst support material in PEM fuel cells also creates opportunities to improve the structure of the catalyst layer although doing so requires consideration of the full range of

catalyst layer properties—ionic transport, charge transport and reactant transport in addition to ECSA. For example, one study has demonstrated an increase of nearly 80% in ECSA by further heat treatment of the catalyst (300 °C, 8 h). However, the fuel cell performance is lower than the untreated one, in which graphene-supported Pt based fuel cell shows a maximum power of 161 mW cm^{-2}.[80] This can be attributed to the loss of proton conductivity of the Nafion® ionomer in the catalyst layer during higher temperature treatment. Another key consideration in the development of graphene-based electrodes is the maintenance of good electronic conductance between graphene layers. As discussed above, nanostructured Pt particles dispersed on functionalized graphene can serve as spacers to prevent the re-agglomeration of graphene sheets. In addition, CNTs can be anchored on the graphene sheet to prevent face-to-face graphene agglomeration while simultaneously increasing the through-plane conductance. Polarization curves for the ORR in a PEM fuel cell electrode using a mix of graphene and CNT supported Pt as electrocatalysts exhibited a performance of 540 mW cm^{-2} for the optimal case of equal fractions of each support (*i.e.* Pt/(50 wt% graphene + 50 wt% CNT).[88] This electrode structure is a combination of functionalized hybrid nanomaterials including three-, two-, and one-dimensional materials. While presenting some advantages, it is likely that the Pt/graphene sheets in this particular architecture pack together to form interstitial pores between the graphene sheets that are relatively inaccessible to electrolyte thus limiting the formation of TPBs. Recently, 3-D Pt-on-Pd bimetallic nanodendrites supported on graphene nanosheets have been constructed, representing a new type of graphene/metal heterostructure.[89] This structure, which exhibits high electrochemically active area, consists of small single-crystal Pt nanoparticles supported on a Pd/graphene nanosheet with porous structure and good dispersion. Electrochemical tests show that the graphene/bimetallic nanodendrite hybrids demonstrate much higher electrocatalytic activity toward methanol oxidation than either platinum black (PB) or commercial E-TEK Pt/C catalysts.[89] Furthermore, as illustrated in Fig. 8, the bimetallic nanodendrites can be applied to construct a novel electrode structure based on graphene nanosheets, which could fully realize the benefit of 2-D graphene while avoiding its disadvantage. The bimetallic nanodendrite hybrid catalyst can be deposited on the graphene sheets. Then, the catalyzed graphene sheets can be assembled onto the PEM in well-ordered macroscopic arrays using directional flow techniques.[8] A very thin ionomer film can then be sprayed onto the arrays to form the ionic pathway. This ideal structure provides for electron transport along the graphene sheet and ion transport in the parallel electrolytic film connecting membrane to reaction sites. In this structure, control of the distance between the graphene sheets is critical to the gas and water transport. Compared to the traditional electrode structure, TPBs are much more accessible as there is no agglomerate structure and catalyst utilization is improved.

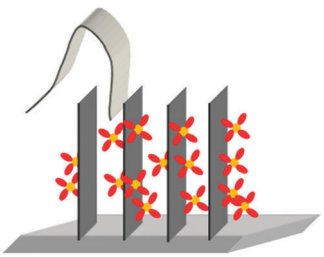

Fig. 8 Strategy for novel electrode structure: bimetallic nanodendrite hybrid catalyzed graphene sheets can be covered by a thin proton ionomer film and assembled on the proton electrolyte membrane.

3.1.4 Emerging applications for graphene in fuel cells. Graphene doped by nitrogen can function as metal-free catalyst for the oxygen reduction reaction (ORR). In a recent study, nitrogen doped graphene (N-graphene) was synthesized by chemical vapor deposition of methane in the presence of ammonia. As illustrated in Fig. 9, the resulting N-graphene shows a much better electrocatalytic activity, long-term operational stability, and tolerance to CO than platinum for the ORR.[90] According to an earlier report on CNTs doped by nitrogen,[91] carbon atoms adjacent to nitrogen dopants possess a substantially high positive charge density to counterbalance the strong electronic affinity of the nitrogen atom. A redox cycling process reduces the carbon atoms that naturally exist in an oxidized form, followed by reoxidation of the reduced carbon atoms to their preferred oxidized state upon O_2 absorption.[91] This is ORR mechanism on the N-doped carbon electrodes. At the same time, the N-induced charge delocalization can change the chemisorption mode of O_2 and weaken the O–O bonding to facilitate ORR at the electrodes. Other work has also demonstrated, enhanced electrochemical activity and durability toward ORR on nitrogen doped graphene.[92] The development of efficient, low cost, and stable N-doped graphene or CNT electrodes capable of replacing the expensive platinum-based electrocatalysts for ORR would be a revolutionary advance in PEM fuel cell technology.

Graphene sheets can also be used as composite fillers and conductive coating in fuel cell application. PEM fuel cell performance can be improved by reducing ohmic losses in the membrane by either increasing ionic conductivity or decreasing thickness of the membrane. Decreasing membrane thickness also facilitates water back diffusion allowing the anode to be operated without external humidification. But, the strength of the membranes becomes lower with the decrease in thickness. As a result, very thin membranes can be reinforced using polytetrafluoroethylene (PTFE) or CNT fillers. Graphene has very high Young's modulus ($\sim$1.0 TPa) and could be used to reinforce the PEMs to dramatically increase their mechanical strength provided electrical shorting through the membrane can be avoided. Another potential application for graphene is as a coating on the bipolar plates to decrease the contact resistance and protect the plate material. Graphene is stable in the fuel cell environment and exhibits high thermal conductivity and electronic conductivity, and thus potentially suitable for this application.

3.2 Supercapacitors

Supercapacitors, also known as ultracapacitors or electrochemical capacitors, electrochemically store and deliver energy at high charge-discharge rates and are a key emerging

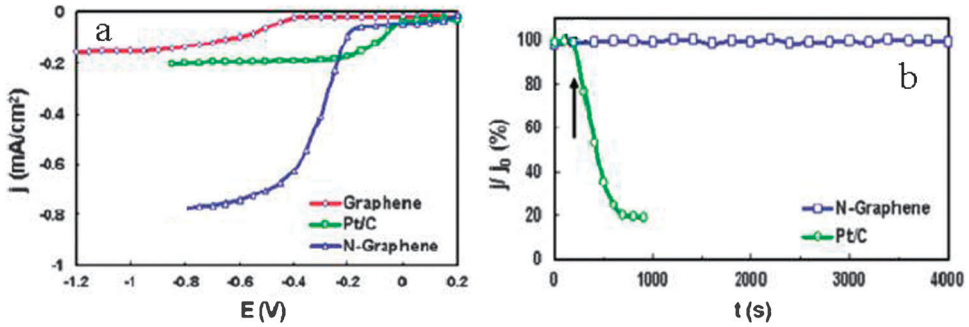

Fig. 9 Electrochemical properties of N-doped graphene: (a) linear scan voltammograms for ORR in air saturated 0.1 M KOH on the electrodes graphene (red), Pt/C (green) and N-doped graphene (blue) with a scan rate of 0.01 V s^{-1} and electrode rotating rate of 1000 rpm; (b) Chronoamperometric response (J_0 the initial current) of Pt/C (circle) and N-doped graphene (square) electrodes to CO and the arrow indicates the addition of 10% CO into air saturated 0.1 M KOH at −0.4 V.[90]

technology for energy storage.[93] Supercapacitors exhibit energy densities several orders of magnitude higher than conventional dielectric capacitors, but still lower than that of batteries. Due to its long cycle life and high power density, a supercapacitor can be used either by itself as the primary power source or in combination with fuel cells or batteries in a wide range of applications such as portable electronics, hybrid electric vehicles and industry backup power. A supercapacitor consists of two electrodes immersed in an electrolyte with a porous separator located between the electrodes. Depending on the charge storage mechanism and the electrode materials used, supercapacitors can be classified as (i) electrochemical double layer capacitors generally using carbon-based electrode materials with high surface area in which fast ion adsorption at the interface of electrode and electrolyte occurs; (ii) pseudo-capacitors based on a Faradic charge transfer process on or near the electrode surface in which transition metal oxides and electrically conducting polymer are used as electrochemically active materials; (iii) a combination of above two types. The energy stored in a supercapacitor, E, can be calculated by $E = 1/2\ CV^2$, in which C is the capacitance and V is the working voltage. Because of the electrochemical decomposition of water, the operating voltage of supercapacitors using aqueous electrolytes like KOH and H_2SO_4 is limited at about 1 V. Greater energy density can be achieved using organic-electrolytes with high working voltages (2.5 to 3.5 V). Even higher working voltage (up to 4.0 V) can be achieved from the ionic liquid electrolytes. The actual performance of the super-capacitor is determined by both the electrochemical activity and the chemical kinetic features of the electrodes. Therefore, it is important to enhance the kinetics of ion and electron transport within the electrodes as well as the charge transfer rate at the interface of electrode and electrolyte.

Graphene has been proposed as an attractive material for supercapacitor applications.[19,94,95] In contrast with conventional high surface area materials, the surface area of individual graphene sheets does not vary with pore size distribution and the graphene sheet exposes both sides to the electrolyte. In graphene, effective surface area is determined by the number of layers of graphene sheets and their stacking configuration. A single layer of graphene with little agglomeration is expected to exhibit high surface area and thus yield higher specific capacitance in a supercapacitor application. However, graphene sheets may stack with each other to form an aggregated structure which may contain open pores. Based on the results of adsorption isotherms and other measurements, adsorption occurs primarily on the surface of graphene sheets with access to large pores contributing to hysteresis loops.[96] In this structure, the presence of a large open pore system within overlayered graphene sheets provides electrolyte ions with easy access to the graphene surfaces where they form double layers. This unique pore structure makes graphene materials very promising in supercapacitors. Performance of graphene based supercapacitors may be further enhanced by: (i) modification of the graphene surface; (ii) hybriding with electrically conductive polymers, and iii) preparation of graphene/metal oxide composites.

As noted previously, although graphene theoretically has a very large specific surface area, the as-prepared specific surface area of actual graphene sheets is reduced by the formation of layers and agglomeration. Several preparation methods have been developed, modified and improved to yield practical graphene sheets with larger specific surface areas. In addition to increasing surface area, the effectiveness of the surface area can be improved by providing surface functional groups on the graphene sheets that provide locations for ion adsorption when in contact with the electrolyte. For example, super-capacitor performance has been shown to improve when graphene is modified with functional groups containing oxygen, nitrogen, boron, and phosphorus as well as doping with nitrogen and boron. Making hybrids of graphene and electrically conducting polymers such as polyaniline (PANI), poly(3,4-ethylenedioxythiophene) (PEDOT) and polypyrrole (PPy) can also increase the supercapacitors performance. Finally, implanting metal oxides (*e.g.* RuO_2, MnO_2, SnO_2 and ZnO_2) with graphene sheets is another effective method. These three methods—surface modification, hybridization, and blending with metal oxides—are described in detail in the following sections.

3.2.1 Graphene modifications. The supercapacitor performance characteristics of graphene are directly related to its as-prepared specific surface area. For example, graphenes, prepared by three different techniques, with surface areas of 925, 520 and 46 $m^2\ g^{-1}$ were shown to exhibit specific capacitances of 117, 35 and 6 F g^{-1} respectively in 1 M

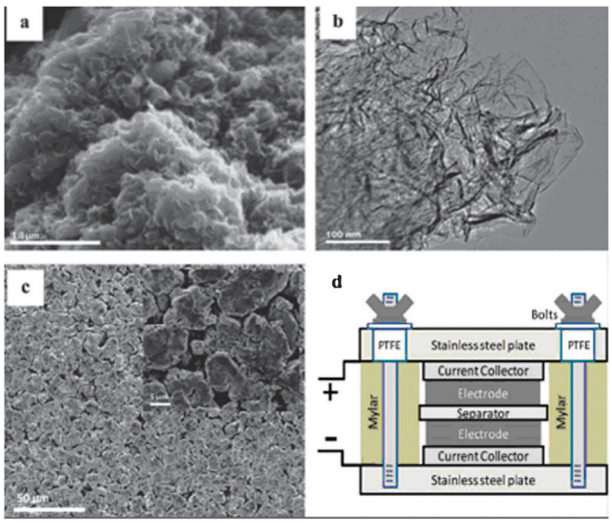

Fig. 10 (a) SEM image of graphene; (b) TEM image showing individual graphene sheets; (c) low and high (inset) magnification SEM images of graphene electrode surface; (d) schematic of cell assembly.[19]

H_2SO_4 solution. The specific capacitance reaches 75 F g^{-1} in the 3.5 V ionic liquid N-butyl-N-methylpyrrolidiniumbis (trifluoromethanesulfonyl) imide ($PYR_{14}TFSI$).[94] As described in section 2, chemical reduction of graphene oxide enables mass production of chemically modified graphene materials with a large quantity of exposed active sites anchored with functional groups. Chemically modified graphene (CMG) was pioneered by Ruoff's group, and specific capacitances of 135 and 99 F g^{-1} in 5M KOH and TEA BF4 in acetonitrile (AN) were respectively demonstrated in supercapacitors (Fig. 10).[19] In addition, the high electrical conductivity of the graphene materials eliminates the need for conductive fillers such as carbon black in the electrode and thus the loading of effective active materials increases, which enables consistently good performance over a wide range of voltage scan rates and simultaneously increases the energy density of the packed supercapacitor. Prolonging the reduction process is an effective method to increase the functional groups on the graphene sheets and thus increase the supercapacitor performance. Graphene materials for supercapacitors have also been reduced from graphene oxide sheets using gas-phase hydrazine, to yield a maximum specific capacitance of 205 F g^{-1} with an energy density of 28.5 Wh kg^{-1} in 30 wt% KOH solution and excellent cycle life, retaining 90% specific capacitance after 1200 cycle tests.[97] Nevertheless, the specific surface area by the Brunauer-Emmett-Teller (BET) method in this study is not large (320 m^2 g^{-1}), and the authors attribute the relatively small area to incomplete removal of the physically adsorbed solvents and the stacking configuration of graphene sheets. It is worthy of noting that the C/N and C/O atomic ratio by elemental analysis is 15.1 and 7.3. Recently, thermal exfoliation at low temperature (200 °C) under high vacuum (<1Pa) was used to prepare graphene sheets for supercapacitor applications. The resulting graphene materials, exhibited a specific surface area of ~400 m^2 g^{-1} based on BET and capacitance as high as 264 F g^{-1} without any post-treatments.[96] The C/O ratio by X-ray photoelectron spectroscopy (XPS) was 10, indicating a large fraction of oxygen containing functional groups was present. A versatile method to simultaneously achieve the exfoliation and reduction of graphite oxide has been applied by microwave assistance.[98] The resulting graphene sheets show a specific surface area of 463 m^2 g^{-1} by BET; a specific capacitance of 191 F g^{-1} in 5M KOH electrolyte; and a C/O ratio of 2.75 by combustion elemental analysis. Though direct comparisons are difficult, a review of the preceding studies suggests that both the specific surface area and the functional groups of graphene materials impact the electrode performance. Another interesting method of graphene preparation for supercapacitors is electrochemical reduction of graphene oxide with extended potential cycling (Fig. 11).[99] The reduction peak at about −0.75 V is ascribed to the electrochemical reduction of graphene oxide. The electrochemically reduced graphene oxide (ER-G) was found to have a specific capacitance of 165 F g^{-1} measured by cyclic voltammetry in 0.1 M Na_2SO_4, much higher than that of CNTs (86 F g^{-1}). Fitting of the high resolution C1s XPS spectra of ER-G suggests numerous oxygen containing groups on the ER-G surface. Since graphene oxide is insulating, the reduction mechanism in the initial cycle is not clear. However, after multiple potential cycles the electrochemical interface or TPB has been established and the surface configuration of the electrode material becomes stable preventing performance degradation during starting charge-discharge cycles.

The influence of post-treatment of graphene surfaces on supercapacitor performance has also been investigated. In this case, the graphene sheets were produced by thermal exfoliation of graphite oxide at relatively low temperature (250–400 °C), and were further treated under N_2 at 700 and 900 °C.[100] Although the BET surface area increases from 404 to 737 m^2 g^{-1} after 900 °C N_2 treatment, the oxygen-containing groups almost disappear during high temperature thermal treatment. Unfortunately, it is found that the specific capacitance of the treated material in 2 M KOH is only 100 F g^{-1} while the one without N_2 treatment shows 230 F g^{-1}. Actually, to investigate the effect of surface functional groups on electrode performance, one should apply careful post-treatment at relatively low temperature (*i.e.* 400 °C). Post-treatment in Ar, N_2, NH_3, H_2, and hydrazine can control the oxygen-containing groups on the graphene sheets by selective removal of oxygen species.[101] In another approach, the effects of oxidant addition

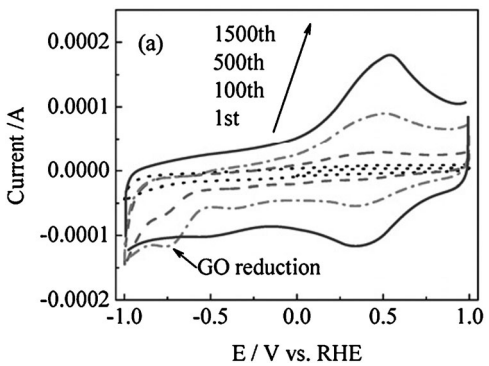

Fig. 11 Cyclic voltammograms for electrochemical reduction of graphene oxide with potential cycling at a scan rate of 50 mV s^{-1} in 0.1 M Na_2SO_4 solution.[99]

on the morphology, structure and electrochemical performance of thermally exfoliated graphene sheets as electrode materials for supercapacitors was systematically investigated. The resulting graphene electrode with a specific surface area of 524 m^2 g^{-1} maintained a stable specific capacitance of 150 F g^{-1} for 500 cycles in 30 wt% KOH.[102] Large concentrations of oxidant applied during the graphite oxidation process can induce numerous oxygen-containing groups, increase the BET specific surface area and significantly lead to more graphene edges, which are favorable for the enhancement of capacitive performance. We believe that the density of lattice defects in the graphene is also enhanced by the harsh processing conditions. If these lattice defects contribute to improved performance, then mechanical milling of the graphene sheets may also be useful to create lattice defects and to increase the ratio of graphene edge to basal surface. Furthermore, the resulting defects and edges may serve to anchor additional functional groups.

A very recent report identifies graphene sheets as the most promising materials for achieving ultrathin and transparent electrodes. Ultrathin and optically transparent graphene films (thin to 25 nm) have been prepared (Fig. 12).[103] The capacitance obtained from charge-discharge analysis is 135 F g^{-1} in 2 M KCl electrolyte for a film of ~25 nm which has a transmittance of 70% at 550 nm. As the authors pointed out, the use of ultrathin transparent graphene films has four advantages: (1) flexible formation of robust film down to 25 nm thick; (2) allowance for supercapacitor application in transparent electronics; (3) elimination of the presence of current collectors which leads to a simplified and lightweight architecture; (4) possibility of enabling graphene to be printed out for full integration with printable electronics.

3.2.2 Graphene-conducting polymer hybrids. Various conducting polymers such as PPy, PANI, PEDOT, polythiophene (PT), and poly(*p*-phenylene vinylene) (PPV) have been investigated as electrode materials or components in supercapacitors due to their high capacitance and relatively easy production. PANI is one of these promising conducting polymers with good environmental stability.[104] Although poor

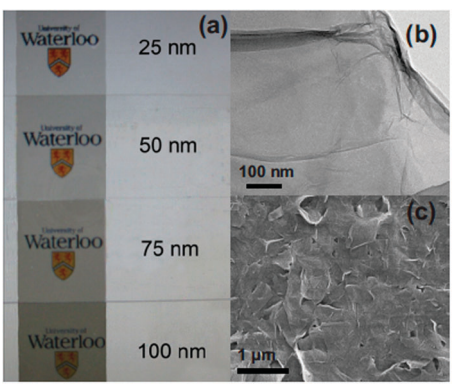

Fig. 12 Morphology of the ultrathin and transparent graphene films: (a) photographs of films on glass substrates; (b) transmission electron microscopy (TEM) images from graphene suspension; (c) scanning electron microscopy (SEM) pictures of 100 nm films on glass substrate.[103]

conductivity usually limits its use in high performance supercapacitors, it can generally promote the electrochemical capacitance of carbon materials and possesses a high doping-dedoping rate during charge-discharge cycles. Therefore, composites based on carbon materials and PANI are generally used as the supercapacitor electrodes. Within these composites, the significance of the specific surface area of the graphene sheets is not nearly as clear. Of more significance in these composite materials is the synergy arising from the interaction of the PANI and graphene materials. Firstly, the addition of graphene sheets can improve the electrical conductivity of PANI and thus can increase its power density. Especially when fully charging or discharging, PANI in its form of leucoemeraldine or pernigranilene is an insulator. The graphene sheets function as the conducting network in the composite materials and improve the electrochemical redox reaction of PANI. Secondly, two charge storage mechanisms including electric double layer charging-discharging of graphene sheets and pseudo-capacitive redox reactions of PANI exist in the composite materials resulting in a higher supercapacitor performance. Most likely, there are still pseudo-capacitive redox reactions of functional groups on graphene sheets. As with most composite materials, the dispersion and composition of the graphene/PANI composite are likely to be critical factors affecting the homogeneous ion accessibility and high interfacial charge storage.

By anodic electropolymerization of 0.05 M aniline monomer on graphene paper, freestanding and flexible graphene/PANI composite papers (GPCPs) have been prepared.[105] Directional flow guided assembly by vacuum infiltration leads to low BET surface area for the graphene paper (94 m^2 g^{-1}). Further, anodic electropolymerization infuses the PANI into the voids of graphene paper, thus decreasing the specific surface area to 39 m^2 g^{-1}. This graphene-based composite paper electrode shows a tensile strength of 12.6 MPa and a large, stable electrochemical capacitance of 233 F g^{-1} (Fig. 13). This capacitance also includes the contribution from the pseudo-capacitive charge storage of functional groups which represent 14 at% concentration based on the XPS analysis.[105] Based on the description of the technique, PANI concentration gradients must exist from the external surface to the interior of the paper, complicating the assessment of the role of PANI in the composite. In another approach to composite electrode fabrication, graphene oxide is used as the filler and the PANI matrix is polymerized *in situ* from the monomer.[106] This approach yields a high specific capacitance of 531 F g^{-1} at a mass ratio of 100 : 1 (aniline/graphite oxide), while individual PANI shows only 216 F g^{-1}. Graphene oxide can be reduced to graphene using reducing agent like hydrazine, and then the reduced PANI can be reoxidized and further reprotonated, which gives rise to graphene/PANI nanocomposites.[107] A uniform nanocomposite with the PANI absorbed on the graphene surface and/or filled between the graphene sheets is observed. Such uniform structure together with the high conductivity affords high specific capacitance of 480 F g^{-1} when the mass ratio of aniline to graphene oxide is 20 : 80. From above examples, it is obvious that either doping PANI in the matrix of graphene based materials or doping graphene based materials in a PANI matrix yields enhanced

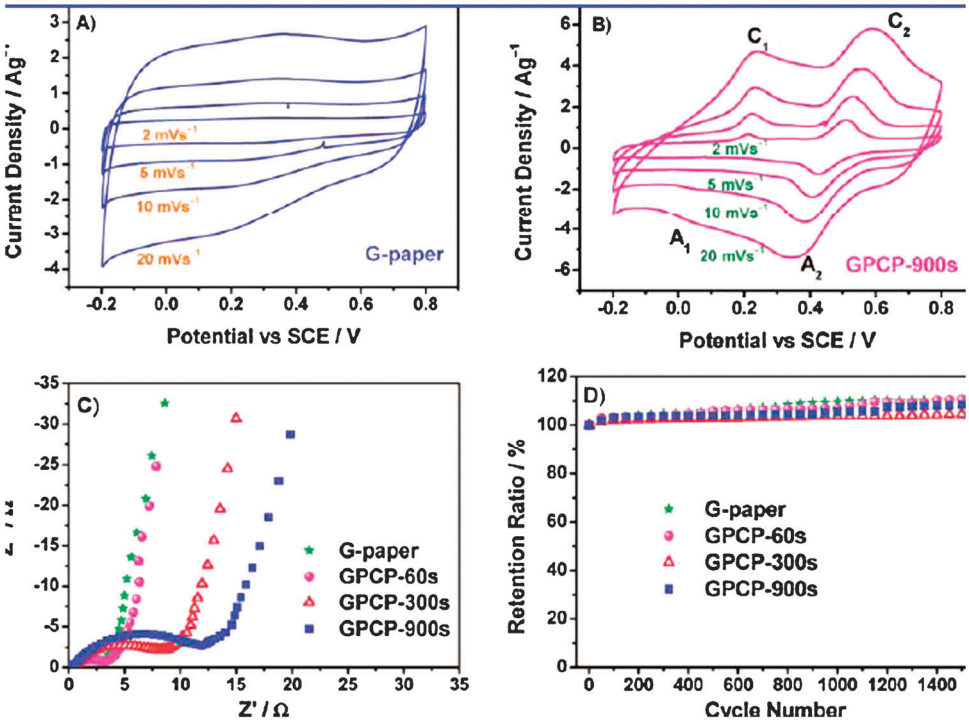

Fig. 13 Electrochemical properties of the graphene paper and GPCP: (a, b) CVs recorded from 2 to 20 mV s^{-1} in 1 M H_2SO_4; (c) Nyquist plots of the graphene paper and GPCP-60s/300s/900s; (d) Cycling performance measured at 50 mV s^{-1}.[105]

supercapacitor performance, which seems attributable to the formation of the unique nanocomposites and/or the interaction between graphene sheets and PANI. Mechanical mixing at the nano or micro scale has been demonstrated as another way to prepare composite films of graphene and PANI. By vacuum-filtering the mixed dispersions of both components, a layered structure of the graphene sheets and PANI nanofibers has been prepared (Fig. 14).[108] The highest specific capacitance and conductivity of the composites are 210 F g^{-1} and 5.5×10^2 S m^{-1} respectively when the composites contain 44% graphene sheets. Unfortunately, this study used graphene sheets with very low specific surface area and yielded a composite with a specific surface area of only 12.7 m^2 g^{-1}. It is possible that the specific capacitance would increase if graphene sheets with high specific surface area had been used instead.

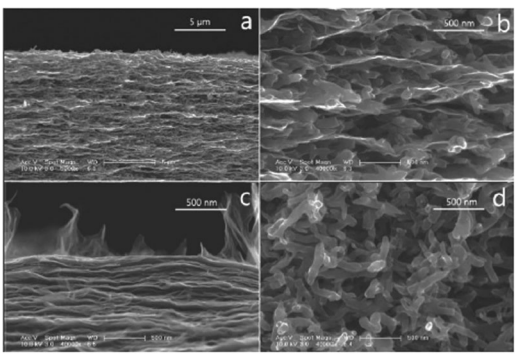

Fig. 14 SEM images of films prepared by vacuum filtration: (a, b) composites of graphene sheets and PANI nanofibers with different magnification; (c) films of pure graphene sheets; (d) films of pure PANI nanofibers.[108]

In supercapacitor applications, the combination of 1-D and 2-D carbon materials can be applied to tune the pore structure of the hybrid films and enhance structural stability. In hybrid films, as with the pure graphene structures described in the preceding section, CNTs can be used to physically separate the graphene sheets to help preserve the high surface area. Using layer-by-layer (LBL) assembly techniques, graphene/CNT hybrid films have been prepared, which possess an interconnected network of carbon structures.[109] Supercapacitors prepared from these films show a specific capacitance of 120 F g^{-1} even at scan rate of 1 V s^{-1}. CNT is also used to prepare graphene/CNT/polyaniline/PANI composite electrodes which exhibit highly conductive pathways as well as improved mechanical strength during doping/dedoping processes.[110]

3.2.3 Graphene—metal oxide composites. Metal oxides such as RuO_2 and Fe_3O_4 have been widely investigated as electrodes for supercapacitors. In addition, the oxides from metal compounds Ti, V, Co, Ni, Zn, Mo, Sn, Ir, *etc.* can also be used as electrode materials in supercapacitors.[93,111] The metal oxides usually possess much larger capacitance than carbon materials due to multi electron transfer during fast Faradaic reactions, which is most attractive for metal oxides. Although RuO_2 demonstrates promising supercapacitive properties, such as high specific capacitance and long cycling stability, its high cost limits its commercialization in supercapacitors. Fe and Mn oxides usually suffer from poor electrical conductivity and relatively short cycling life. Inspired by electrode preparation in fuel cells and lithium ion batteries, there are three main improvement strategies for metal oxides

as supercapacitor electrodes. First, nanostructuring of metal oxides involves decreasing the particle size and increasing its specific surface area to create a larger interface between the electrode and electrolyte. Decreasing the particle size also reduces the path length for electronic transport thus counteracting the poor electrical conductivity of their bulk metal oxides. Nanostructuring can also, to some extent, lead to better accommodation of strain during cycle life, thus improving the stability of electrode materials. A second approach is functionalization of metal oxide surfaces. For example application of a mixed conducting film can facilitate the proton exchange process that usually accompanies the electron transfer process. Finally, the metal oxide particles can be supported on carbonaceous materials like graphene.

Metal oxides supported on carbonaceous materials like graphene can maintain constant or superior electrochemical performance while the metal oxide loading decreases. The carbon materials provide an electrically conductive filler which facilitates the formation of a conductive network which is essential to the poor conducting metal oxides. In addition, the carbon materials also function directly as electrode materials based on the electrochemical double layer charge storage mechanism. A one-step method was developed to fabricate conductive graphene/SnO_2 nanocomposites in acidic solution, in which graphite oxides were reduced by $SnCl_2$ to graphene sheets in the presence of HCl and urea.[112] Despite the improved electrical conductivity and high graphene surface area, the specific capacitance of this composite in 1 M H_2SO_4 is only 43.4 F g^{-1}. In another approach, ultrasonic pyrolysis of ZnO onto graphene has been used to produce graphene–metal oxide composite films that have been successfully used as electrode materials for electrochemical supercapacitors.[113,114] Although the specific capacitance for graphene–ZnO and graphene–SnO_2 is not high (61.7 and 42.7 F g^{-1} respectively) compared with those from the composites of graphene and PANI, the metal oxide composites exhibit an enhanced capacitive behavior and improved charge-discharge behavior when compared to pure graphene or pure metal oxide electrodes. The metal oxide, MnO_2, has attracted a great deal of interest as a supercapacitor electrode due to high specific capacitance, environmental compatibility and cost effectiveness.[115] A composite of graphene oxide supported by needle-like MnO_2 nanocrystals (GO–MnO_2 nanocomposites) has been fabricated in a water-isopropyl alcohol system.[116] The specific capacitances for GO–MnO_2, nano MnO_2, GO in 1 M Na_2SO_4 are measured as 197.2, 211.2 and 10.9 F g^{-1}. According to the ratio of MnO_2 to GO in GO–MnO_2 (9.8/1), theoretical specific capacitance assuming proportional contribution from each component is thus 192.7 F g^{-1} which is very close to the measured value (197.2 F g^{-1}). These results seem to suggest that the electrochemical performance of this particular nanocomposites is not enhanced by any interaction between GO and MnO_2. Some hydroxides, due to well defined redox reactions and low cost, have also been applied to make composites with graphene sheets to increase the specific capacitance. Single-crystalline $Ni(OH)_2$ hexagonal nanoplates have been directly grown on graphene sheets, and found to exhibit a very high specific capacitance of $\sim$1335 F g^{-1} (Fig. 15).[117] In contrast to the GO–MnO_2 nanocomposites, a simple physical mixture of pre-synthesized $Ni(OH)_2$ nanoplates and graphene sheets shows a lower specific capacitance. This suggests that the interaction between nanoparticles and graphene may be important and may affect the charge transport from nanparticles to conducting graphene network. In addition, graphene–$Co(OH)_2$ nanocomposites have been synthesized by using precursor Na_2S in water and isopropanol, in which the deposition of Co^{2+} and the reduction of graphene oxide occur at the same time[118] It is found that the specific capacitance of the nanocomposites reaches 972.5 F g^{-1}, remarkably higher than each individual counterpart (137.6 and 726.1 F g^{-1} for graphene and $Co(OH)_2$). This again indicates nancomposites exhibit a synergistic effect. These conflicting reports regarding the presence or absence of synergistic effects within graphene metal-oxide nanocomposites will likely lead to further study of graphene based nanocomposites and perhaps to improved supercapacitor performance. Specific questions that may warrant further study in this area include: Does the feeding ratio of nanoparticles to graphene have a pronounced effect on its electrochemical activities? Is the electrochemical performance of these composites dependent on the graphene quality and the morphology and crystallinity of the nanomaterials? How will the specific surface area of graphene and functional groups influence the composites properties?

3.2.4 Macroscopic structure. For supercapacitors in practical applications, the replacement of powders and binders with a robust macroscopic/monolithic structure is preferable. At present, macroscopic binderless fabrication of graphene-based materials has already been demonstrated for supercapacitor applications.[119,120] In such kind of structure, the porous materials, for example, Ni-fiber,[119] carbon cloth and carbon paper[120] are chosen as substrates and layers of graphene are deposited on by CVD. These graphene layers can form carbon nano-fibers (CNFs) with mesopores structure and can be predominantly vertically oriented with respect to a substrate.[119,120] One of the most promising is the use as electrodes in supercapacitors, and this hybrid structure shows good capacitive behavior. Proper combination of cathode and anode can increase the working voltage of supercapacitors, and as a result increase power and energy densities. An asymmetric hybrid supercapacitor combines PANI nanofibers as cathode (0.2–0.7 V *vs.* Ag/AgCl) and graphene as anode (−0.3–0.2 V *vs.* Ag/AgCl), and shows the energy and power densities of 4.86 Wh kg^{-1} and 8.75 kW kg^{-1}, respectively.[121]

3.3 Lithium ion batteries

The lithium ion battery (LIB) was commercialized by the Sony Company in the early 1990s, and owing to its high voltage, high energy density, long cycling life, light weight and good environmental compatibility it has become the most important secondary battery for various portable electronic device applications.[122,123] A LIB consisting generally of an anode or negative electrode, cathode or positive electrode, and electrolyte (separator) is an electrochemical energy storage device based on intercalation and deintercalation of lithium ions. When charging, the lithium ions are extracted from the cathode and introduced into the anode. When discharging, the

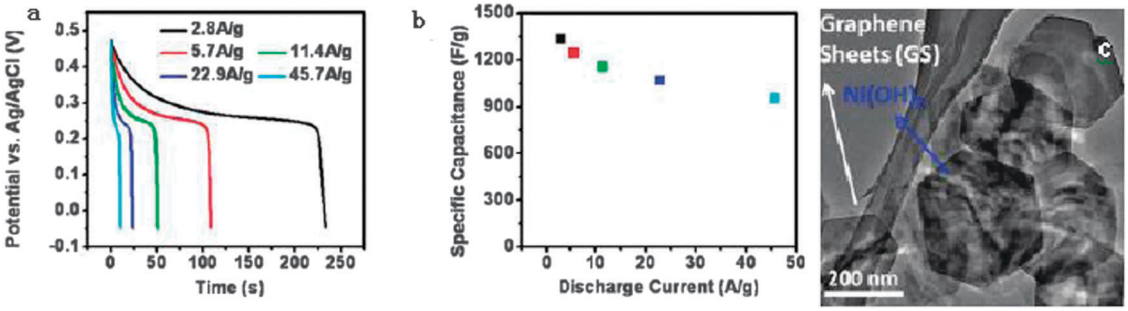

Fig. 15 (a) Galvanostatic discharge curves of $Ni(OH)_2$ grown on graphene sheets at different discharge current densities; (b) Average specific capacitance for $Ni(OH)_2$ grown on graphene sheets at different discharge current densities; (c) TEM image of $Ni(OH)_2$ grown on graphene sheets.[117]

reverse happens. Usually, the anode is comprised of materials that can reversibly store lithium ions *e.g.*, carbon, transition metal oxides and alloying materials such as Si and Sn. The cathode materials are typically Li-containing metal oxides like lithium cobalt oxide and lithium iron phosphate. Compared with supercapacitors, the electrode requirements are much more demanding in batteries. The effect of carbonaceous electrode structure (layered, ordered, and disordered) on battery performance has been reviewed previously.[124] Here, we will summarize the recent work exploring the use of graphene as (i) graphene anodes; (ii) graphene-based hybrid anodes; and iii) electrode additives to enhance performance.

3.3.1 Graphene anodes. Graphitic carbon is widely used as an anode material in LIBs, but exhibits low Li storage capacity (*i.e.* less than 372 mA h g^{-1}). The low storage capacity of graphite is ascribed to limited Li ion storage sites within the sp^2 carbon hexahedrons—typically one per hexahedron yielding LiC_6. Two configurations have been proposed to go beyond the limitation of the LiC_6 configuration: one is the double layer adsorption[125] configuration and another is the covalent molecule configuration.[126] In the former case, both planes of a graphene sheet adsorb Li ions, yielding Li_2C_6 with a Li storage capacity of $\sim$780 mA h g^{-1}. In the latter case, each Li atom is trapped at a covalent site on the benzene ring and therefore the highest Li storage capacity corresponds to LiC_2 and is $\sim$1116 mA h g^{-1}. Obviously a single layer of graphene in the LiC_6 configuation is not a promising insertion material, but attainment of the double-layer or covalent configuration could yield attractive performance.

Another idea is to reassemble each single graphene sheet with spacers to achieve "pseudo-graphite" with a large interlayer distance; so that more Li ions can be stored in between the graphene interlayers thus leading to a high capacity. By carefully controlling the layer spacing between the reassembled graphene nanosheets through interacting molecules such as CNTs and fullerenes, the specific capacity of graphene nanosheets (GNS) increases from 540 mAh g^{-1}, to 730 mAh g^{-1} with CNT incorporation and to 784 mAh g^{-1} with C-60 incorporation.[127] However, the battery shows poor cyclic performance as the capacity drops from 540 mAh g^{-1} to 290 mAh g^{-1} after only 20 charge-discharge cycles. Nevertheless, the demonstration of graphene as a potential anode material supports the need for further research into other methods for fabricating graphene anodes. In one alternative method, graphene paper can be prepared by flow-directed vacuum filtration and hydrazine reduction of prefabricated graphene oxide paper. The distance between the resulting graphene layers is $\sim$0.375 nm, larger than that of graphite (0.334 nm).[128,129] Although this material exhibits a dramatic capacity drop from 680 to 84 mA h g^{-1} after the first cycle, a comparatively flat discharge plateau exists at 2.20 V in the first discharge curve with a discharge capacity of 582 mA h g^{-1}. This raises the possibility of using graphene paper in a new primary battery system.[128] The advantage of using graphene paper as an electrode is that it is applicable as a single electrochemically active component without the need for polymer binders and other additives that are required for the fabrication of conventional electrodes.[129] Another novel method has been used to control the distance between graphene layers. In this method, the graphene sheets are functionalized by oxalic acid molecules, poly-condensed under the evolution of water via oxalyl bonding and assembled along the tubular axis of templating CNTs, forming layered co-axial tubes.[130] The interstitial inclusion of moieties increases the interlayer distance from $\sim$0.339 nm to 0.378 nm, which results in a reversible capacity of $\sim$375 mA h g^{-1}. However, the irreversible capacity losses during the first cycle and poor cyclic performance for the graphene based electrode are problematic and will require further work to identify the cause and to suggest potential solutions. These types of material systems are strongly influenced by: the spacing of d (002) within the graphene sheets; specific surface area; functional groups on the graphene; and defects.[131] The beneficial capacity increase arising from the use of graphene instead of graphite is caused by the expansion of the interlayer spacing of the graphene sheets, which improves the insertion storage. In addition, defects in the graphene also contribute, and high reversible capacities (794–1054 mA h/g) and good cyclic stability were reported.[131] It is likely that defects such as edge defects and vacancies also enhance reversible capacity in disordered graphene nanosheets.[129] On the other hand, the irreversible capacity loss is generally attributed to the presence of oxygen-containing functional groups which lead to the formation of a solid electrolyte interface (SEI) film and to the reaction of Li ions with these groups.[132] Modeling work based on density functional theory (DFT) has shown that the introduction of armchair and zigzag edges leads to enhanced

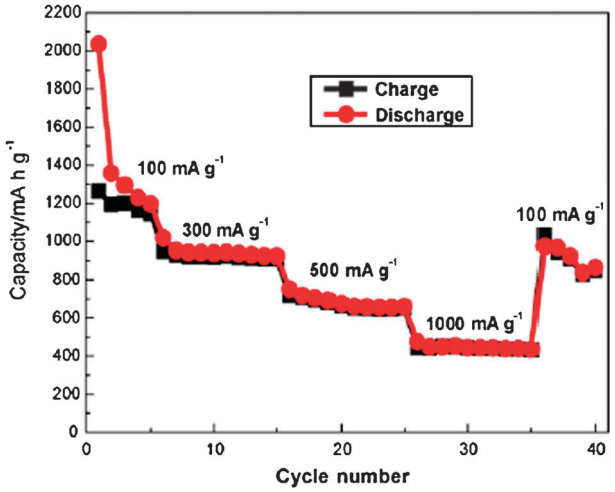

Fig. 16 Cycle performance for graphene anode at the current densities from 100 to 1000 mA h g^{-1}.[135]

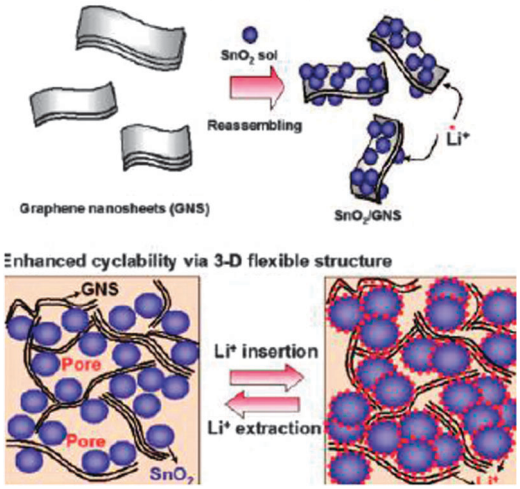

Fig. 17 The structure of hybrids including metal oxides such as SnO_2 and graphene sheets which enhances the cycle performance of electrodes.[136]

adsorption of Li ions and enhanced diffusion properties.[133] This theoretical research suggests that if a graphene nanoribbon is used as the anode material, the advantage of enhanced adsorption of Li ions and their increased diffusion rate can be fully exploited. Another benefit to the use of small graphene sheets like graphene nanoribbons is that the diffusion distance of Li ions can be reduced, which makes the reaction rate of intercalation and deintercalation much faster. To fully realize this benefit, the graphene sheets must be oriented in a direction that facilitates Li ion insertion and extraction. Otherwise, nano-holes must exist on the graphene sheets, which is unlikely, although such nano-holes have been proposed in the basal graphene plane on the round-shaped natural graphite.[134] Recently, anodes were fabricated from high quality graphene sheets (approximately 4 layers with a specific surface area of 492.5 m^2 g^{-1}) prepared by oxidation of graphite powder followed by rapid thermal expansion in nitrogen atmosphere.[135] The initial reversible specific capacity of the prepared graphene sheets was as high as 1264 mA h g^{-1} at a current density of 100 mA h g^{-1}. After 40 cycles, the reversible capacity was still 848 mA h g^{-1} (Fig. 16).

3.3.2 Graphene based heterogeneous hybrids. Transition metal oxides can reversibly react with Li ions and thus can provide Li storage capability. For example, SnO_2 has high theoretical Li storage capacity of 782 mA h g^{-1}, much higher than that of graphite. Unfortunately during charge-discharge cycles, SnO_2 experiences a very large volume change which causes crumbling and cracking of the electrodes resulting in poor cyclic performance. To circumvent these problems, graphene nanosheets in an ethylene glycol solution can be reassembled in the presence of rutile SnO_2 nanoparticles (Fig. 17).[136] The graphene nanosheets are homogeneously distributed between the SnO_2 nanoparticles in such a way that a nanoporous structure with a large amount of void space is prepared. The dimensional confinement of SnO_2 nanoparticles by the surrounding graphene sheets limits the volume expansion upon Li insertion, and the pores between SnO_2 and graphene sheets can be used as buffering spaces during charge–discharge cycles, leading to improved cyclic performances.[136] Co_3O_4, due to its high theoretical capacity (890 mA h g^{-1}), has also been anchored on graphene sheets as an advanced anode material.[137,138] In these hybrid materials, the graphene sheets not only provide buffering spaces but also prevent the agglomeration of Co_3O_4 nanoparticles. In addition, the graphene sheets in the hybrids serve as the electrical conducting network to improve the power density of the electrodes. The graphene sheets themselves also work as electrode materials for Li ion storage. Finally, the metal oxide particles between graphene sheets effectively prevent agglomeration of graphene sheets and keep them available to Li insertion and extraction. This final effect also maintains a large specific surface area that may have the negative effect of inducing high irreversible capacity loss during the first charge-discharge cycle due to the formation of SEI films.[131] The net effect on long term performance is an area for further research. In addition to the homogeneous graphene/metal oxide mixtures, self-assembly methods directed by surfactants or polymers have been used to construct ordered metal oxide-graphene nanocomposites.[139] In such layered nanocomposites, stable alternating layers of nanocrystalline metal oxides with graphene or graphene stacks are formed.

The elements Sn and Si can reversibly react with Li forming Li alloys that have very high theoretical capacities of 993 and 4200 mA h g^{-1} respectively. As with the transition metal oxides, large volume expansion occurs once Li intercalates into these elements limiting the battery lifetime. A general strategy has been demonstrated to achieve improved electrochemical performance by constructing 3D nanocomposite architectures based on the combination of nanosize Sn particles and graphene nanosheets.[140] Electrochemical tests demonstrate the highly reversible nature of the reaction between Li^+ and Sn/graphene nanocomposites. In this study, Li can be stably stored on both sides of graphene sheets (Li_2C_6) with a theoretical capacity of 744 mA h g^{-1} predicted from first principles. For Si, it has been demonstrated that enhanced cyclic performance can be achieved in electrodes prepared by simple mixing of commercially available nanosize

Si and graphene.[141] After 30 cycles the mixed Si/graphene composite retains a capacity of 1168 mA h g^{-1} and an average coulombic efficiency of 93%. Composites consisting of Si nanoparticles and graphene paper have also demonstrated high Li ion storage capacities and cycling stability with storage capacity $>$ 2200 mA h g^{-1} after 50 cycles and $>$ 1500 mA h g^{-1} after 200 cycles with a decrease rate of $\sim$0.5% per cycle.[142] From these results, the benefits of using graphene based hybrids are obvious. However, in spite of promising early results, considerably more work is needed to systematically compare the performance of graphene based materials to other carbonaceous materials and to establish a level of understanding that can lead to optimal graphene composite electrodes.

3.3.3 Electrode additive. Graphene has excellent electrical conductivity and is an ideal conductive additive in hybrid nanstructured electrodes. Nanostructured TiO_2-graphene prepared by a self-assembly technique shows significantly enhanced Li-ion insertion/extraction compared with pure TiO_2. The doubled specific capacity as compared with the pure TiO_2 phase and the improved capacity at high charge-discharge rate may be attributed to increased electrode conductivity in the presence of a percolated graphene network embedded into the metal oxide electrodes.[139] Later, this anatase TiO_2/graphene composite anode was combined with the $LiFePO_4$ cathode to form a full cell that operated at 1.6 V and demonstrated negligible fade even after more than 700 cycles at a one-hour discharge rate.[143] This battery potentially offers long life and low cost, along with safety, all of which are critical to the stationary and vehicle applications. In another study, $LiFePO_4$/graphene composites were prepared by the co-precipitation method, and the capacity and cycle performances of $LiFePO_4$ were improved considerably.[144] Graphene has also been shown to improve the performance of $Li_4Ti_5O_{12}$ (LTO) anodes for LIBs. While LTO anodes are advantageous due to their well-known zero-strain characteristics, the electrical conductivity of LTO is intrinsically poor, and graphene can be an effective additive to improve the surface conductivity of the nanocomposites.[145] In this study, the as-prepared graphene-embedded LTO anode material showed improved charge/discharge rates and cyclic durability, particularly at high rates (*e.g.* 22 °C rate), which makes the nanocomposite an attractive anode material for applications in electric vehicles.

4. Remarks and perspective

In the field of electrochemical energy conversion and storage, graphene has shown promise for applications in fuel cells, supercapacitors and lithium ion batteries. Due to its specific surface area and the presence of functional groups, edges and defects, graphene-based electrodes demonstrate enhanced performance for such electrochemical energy devices. Early examples of improvements achieved with graphene include: (i) the interactions between graphene and supported catalyst particles have been shown to improve the catalyst durability for fuel cells; (ii) hybrids of graphene and metal oxides or graphene and conducting polymers as have demonstrated synergic effects for supercapacitor applications; and (iii) the combination of graphene with lithium storage materials has yielded increased electrode capacity. However, the development of graphene materials and their application in the electrochemical energy fields is still in its infancy and many challenges remain. Well controlled methods of synthesis and processing of graphene based materials are only beginning to emerge. A better understanding of the correlation between the electrochemical performance and graphene structures, properties and interactions within hybrids is needed.

Further work should include pursuing the most suitable methods for preparing graphene for electrochemical applications. Methods to control the number of layers, the extent of defects, and the surface functionality must be developed and tailored to specific applications. Also, early successes warrant continued exploration of the synthesis of graphene-based electrode materials with high electrochemical performance, for example, graphene supported precious or non-precious metals and binary catalysts with high activity and stability that may have application to alcohol oxidation or oxygen reduction. In addition, current electrode designs should be revisited to explore whether graphene with its unique structure and properties may enable enhanced performance. For example, the development of a novel and effective battery electrode based on nano-sized lithium storage materials, may be possible using graphene to create an aligned structure that facilitates Li ion insertion and extraction while also facilitating good electrical conductivity within the electrode. Finally, a more fundamental understanding of the chemical and physical mechanisms that give rise to the electrochemical properties of graphene-based structures is essential. This effort will require experimental work to systematically vary surface area, functional groups, and defects to explore the resulting effect on properties as well as analytical work to reconcile observations with physical principles.

Acknowledgements

The author Hou would like to thank Dr Min Yang for valuable discussions.

References

1 K. S. Novoselov, *et al.*, Electric field effect in atomically thin carbon films, *Science*, 2004, **306**(5696), 666–669.
2 A. K. Geim and K. S. Novoselov, The rise of graphene, *Nat. Mater.*, 2007, **6**(3), 183–191.
3 A. K. Geim, Graphene: Status and Prospects, *Science*, 2009, **324**(5934), 1530–1534.
4 C. Lee, *et al.*, Measurement of the elastic properties and intrinsic strength of monolayer graphene, *Science*, 2008, **321**(5887), 385–388.
5 A. A. Balandin, *et al.*, Superior thermal conductivity of single-layer graphene, *Nano Lett.*, 2008, **8**(3), 902–907.
6 S. Stankovich, *et al.*, Graphene-based composite materials, *Nature*, 2006, **442**(7100), 282–286.
7 T. Ramanathan, *et al.*, Functionalized graphene sheets for polymer nanocomposites, *Nat. Nanotechnol.*, 2008, **3**(6), 327–331.
8 D. A. Dikin, *et al.*, Preparation and characterization of graphene oxide paper, *Nature*, 2007, **448**(7152), 457–460.
9 K. S. Kim, *et al.*, Large-scale pattern growth of graphene films for stretchable transparent electrodes, *Nature*, 2009, **457**(7230), 706–710.
10 A. Reina, *et al.*, Large area, few-layer graphene films on arbitrary substrates by chemical vapor deposition, *Nano Lett.*, 2009, **9**(1), 30–35.

11 Y. M. Shi, *et al*., Work function engineering of graphene electrode via chemical doping, *ACS Nano*, 2010, **4**(5), 2689–2694.
12 X. S. Li, *et al*., Transfer of large-area graphene films for high-performance transparent conductive electrodes, *Nano Lett*., 2009, **9**(12), 4359–4363.
13 J. S. Bunch, *et al*., Electromechanical resonators from graphene sheets, *Science*, 2007, **315**(5811), 490–493.
14 C. Y. Chen, *et al*., Performance of monolayer graphene nanomechanical resonators with electrical readout, *Nat. Nanotechnol*., 2009, **4**(12), 861–867.
15 F. Schedin, *et al*., Detection of individual gas molecules adsorbed on graphene, *Nat. Mater*., 2007, **6**(9), 652–655.
16 D. C. Elias, *et al*., Control of graphene's properties by reversible hydrogenation: Evidence for graphane, *Science*, 2009, **323**(5914), 610–613.
17 C. S. Shan, *et al*., Direct electrochemistry of glucose oxidase and biosensing for glucose based on graphene, *Anal. Chem*., 2009, **81**(6), 2378–2382.
18 R. Balog, *et al*., Bandgap opening in graphene induced by patterned hydrogen adsorption, *Nat. Mater*., 2010, **9**(4), 315–319.
19 M. D. Stoller, *et al*., Graphene-based ultracapacitors, *Nano Lett*., 2008, **8**(10), 3498–3502.
20 J. C. Meyer, *et al*., The structure of suspended graphene sheets, *Nature*, 2007, **446**(7131), 60–63.
21 X. Du, *et al*., Approaching ballistic transport in suspended graphene, *Nat. Nanotechnol*., 2008, **3**(8), 491–495.
22 A. Shukla, *et al*., Graphene made easy: High quality, large-area samples, *Solid State Commun*., 2009, **149**(17–18), 718–721.
23 Y. Hernandez, *et al*., High-yield production of graphene by liquid-phase exfoliation of graphite, *Nat. Nanotechnol*., 2008, **3**(9), 563–568.
24 M. Lotya, *et al*., Liquid phase production of graphene by exfoliation of graphite in surfactant/water solutions, *J. Am. Chem. Soc*., 2009, **131**(10), 3611–3620.
25 C. A. Furtado, *et al*., Debundling and dissolution of single-walled carbon nanotubes in amide solvents, *J. Am. Chem. Soc*., 2004, **126**(19), 6095–6105.
26 U. Khan, *et al*., High-concentration solvent exfoliation of graphene, *Small*, 2010, **6**(7), 864–871.
27 J. N. Coleman, Liquid-phase exfoliation of nanotubes and graphene, *Adv. Funct. Mater*., 2009, **19**(23), 3680–3695.
28 C. Berger, *et al*., Ultrathin epitaxial graphite: 2D electron gas properties and a route toward graphene-based nanoelectronics, *J. Phys. Chem. B*, 2004, **108**(52), 19912–19916.
29 C. Berger, *et al*., Electronic confinement and coherence in patterned epitaxial graphene, *Science*, 2006, **312**(5777), 1191–1196.
30 T. Ohta, *et al*., Controlling the electronic structure of bilayer graphene, *Science*, 2006, **313**(5789), 951–954.
31 J. Coraux, *et al*., Structural coherency of graphene on Ir(111), *Nano Lett*., 2008, **8**(2), 565–570.
32 P. W. Sutter, J. I. Flege and E. A. Sutter, Epitaxial graphene on ruthenium, *Nat. Mater*., 2008, **7**(5), 406–411.
33 X. S. Li, *et al*., Large-area synthesis of high-quality and uniform graphene films on copper foils, *Science*, 2009, **324**(5932), 1312–1314.
34 C. D. Kim, B. K. Min and W. S. Jung, Preparation of graphene sheets by the reduction of carbon monoxide, *Carbon*, 2009, **47**(6), 1610–1612.
35 A. G. Cano-Marquez, *et al*., Ex-MWNTs: Graphene sheets and ribbons produced by lithium intercalation and exfoliation of carbon nanotubes, *Nano Lett*., 2009, **9**(4), 1527–1533.
36 D. V. Kosynkin, *et al*., Longitudinal unzipping of carbon nanotubes to form graphene nanoribbons, *Nature*, 2009, **458**(7240), 872.
37 A. Sinitskii, *et al*., Corrugation of chemically converted graphene monolayers on SiO2, *ACS Nano*, 2010, **4**(6), 3095–3102.
38 L. Y. Jiao, *et al*., Narrow graphene nanoribbons from carbon nanotubes, *Nature*, 2009, **458**(7240), 877–880.
39 H. C. Schniepp, *et al*., Functionalized single graphene sheets derived from splitting graphite oxide, *J. Phys. Chem. B*, 2006, **110**(17), 8535–8539.
40 M. J. McAllister, *et al*., Single sheet functionalized graphene by oxidation and thermal expansion of graphite, *Chem. Mater*., 2007, **19**(18), 4396–4404.
41 A. V. Murugan, T. Muraliganth and A. Manthiram, Rapid, facile microwave-solvothermal synthesis of graphene nanosheets and their polyaniline nanocomposites for energy strorage, *Chem. Mater*., 2009, **21**(21), 5004–5006.
42 Z. T. Luo, *et al*., High yield preparation of macroscopic graphene oxide membranes, *J. Am. Chem. Soc*., 2009, **131**(3), 898.
43 W. F. Chen, L. F. Yan and P. R. Bangal, Preparation of graphene by the rapid and mild thermal reduction of graphene oxide induced by microwaves, *Carbon*, 2010, **48**(4), 1146–1152.
44 M. Choucair, P. Thordarson and J. A. Stride, Gram-scale production of graphene based on solvothermal synthesis and sonication, *Nat. Nanotechnol*., 2008, **4**(1), 30–33.
45 X. L. Li, *et al*., Chemically derived, ultrasmooth graphene nanoribbon semiconductors, *Science*, 2008, **319**(5867), 1229–1232.
46 S. Gilje, *et al*., A chemical route to graphene for device applications, *Nano Lett*., 2007, **7**(11), 3394–3398.
47 S. Park and R. S. Ruoff, Chemical methods for the production of graphenes, *Nat. Nanotechnol*., 2009, **4**(4), 217–224.
48 L. Zhang, *et al*., Controlled synthesis of few-layered graphene sheets on a large scale using chemical exfoliation, *Carbon*, 2010, **48**(8), 2367–2371.
49 D. Li, *et al*., Processable aqueous dispersions of graphene nanosheets, *Nat. Nanotechnol*., 2008, **3**(2), 101–105.
50 W. S. Hummers and R. E. Offeman, Preparation of graphitic oxide, *J. Am. Chem. Soc*., 1958, **80**, 1339.
51 S. Stankovich, *et al*., Synthesis of graphene-based nanosheets via chemical reduction of exfoliated graphite oxide, *Carbon*, 2007, **45**(7), 1558–1565.
52 Y. Si and E. T. Samulski, Synthesis of water soluble graphene, *Nano Lett*., 2008, **8**(6), 1679–1682.
53 X. B. Fan, *et al*., Deoxygenation of exfoliated graphite oxide under alkaline conditions: a green route to graphene preparation, *Adv. Mater*., 2008, **20**(23), 4490–4493.
54 X. C. Dong, *et al*., Ultra-large single-layer grapheneobtained from solution chemical reduction and its electrical properties, *Phys. Chem. Chem. Phys*., 2010, **12**(9), 2164–2169.
55 S. Niyogi, *et al*., Solution properties of graphite and graphene, *J. Am. Chem. Soc*., 2006, **128**(24), 7720–7721.
56 J. F. Che, L. Y. Shen and Y. H. Xiao, A new approach to fabricate graphene nanosheets in organic medium: combination of reduction and dispersion, *J. Mater. Chem*., 2010, **20**(9), 1722–1727.
57 J. Liu, *et al*., Reduction of functionalized graphite oxides by trioctylphosphine in non-polar organic solvents, *Carbon*, 2010, **48**(8), 2282–2289.
58 X. R. Wang, *et al*., N-doping of graphene through electrothermal reactions with ammonia, *Science*, 2009, **324**(5928), 768–771.
59 D. B. Farmer, *et al*., Chemical doping and electron-hole conduction asymmetry in graphene devices, *Nano Lett*., 2009, **9**(1), 388–392.
60 L. Ci, *et al*., Atomic layers of hybridized boron nitride and graphene domains, *Nat. Mater*., 2010, **9**(5), 430–435.
61 A. Kasry, *et al*., Chemical doping of large-area stacked graphene films for use as transparent, conducting electrodes, *ACS Nano*, 2010, **4**(7), 3839–3844.
62 J. M. Cai, *et al*., Atomically precise bottom-up fabrication of graphene nanoribbons, *Nature*, 2010, **466**(7305), 470–473.
63 Z. S. Wu, *et al*., Synthesis of graphene sheets with high electrical conductivity and good thermal stability by hydrogen arc discharge exfoliation, *ACS Nano*, 2009, **3**(2), 411–417.
64 J. Geng, *et al*., Preparation of graphene relying on porphyrin exfoliation of graphite, *Chem. Commun*., 2010, **46**(28), 5091–5093.
65 Q. Y. He, *et al*., Centimeter-long and large-scale micropatterns of reduced graphene oxide films: fabrication and sensing applications, *ACS Nano*, 2010, **4**(6), 3201–3208.
66 W. F. Zhao, *et al*., Preparation of graphene by exfoliation of graphite using wet ball milling, *J. Mater. Chem*., 2010, **20**(28), 5817–5819.
67 R. S. Sundaram, *et al*., Electrochemical modification of graphene, *Adv. Mater*., 2008, **20**(16), 3050–3053.
68 C. N. R. Rao, *et al*., Graphene: The new two-dimensional nanomaterial, *Angew. Chem., Int. Ed*., 2009, **48**(42), 7752–7777.
69 L. H. Tang, *et al*., Preparation, structure, and electrochemical properties of reduced graphene sheet films, *Adv. Funct. Mater*., 2009, **19**(17), 2782–2789.
70 M. Zhou, Y. M. Zhai and S. J. Dong, Electrochemical sensing and biosensing platform based on chemically reduced graphene oxide, *Anal. Chem*., 2009, **81**(14), 5603–5613.

71 R. L. McCreery, Advanced carbon electrode materials for molecular electrochemistry, *Chem. Rev.*, 2008, **108**(7), 2646–2687.
72 M. Pumera, Electrochemistry of graphene: new horizons for sensing and energy storage, *Chem. Rec.*, 2009, **9**(4), 211–223.
73 B. C. H. Steele and A. Heinzel, Materials for fuel-cell technologies, *Nature*, 2001, **414**(6861), 345–352.
74 R. Borup, *et al.*, Scientific aspects of polymer electrolyte fuel cell durability and degradation, *Chem. Rev.*, 2007, **107**(10), 3904–3951.
75 Y. Y. Shao, G. P. Yin and Y. Z. Gao, Understanding and approaches for the durability issues of Pt-based catalysts for PEM fuel cell, *J. Power Sources*, 2007, **171**(2), 558–566.
76 C. Xu, X. Wang and J. W. Zhu, Graphene-Metal Particle Nanocomposites, *J. Phys. Chem. C*, 2008, **112**(50), 19841–19845.
77 Y. M. Li, L. H. Tang and J. H. Li, Preparation and electrochemical performance for methanol oxidation of pt/graphene nanocomposites, *Electrochem. Commun.*, 2009, **11**(4), 846–849.
78 S. Sharma, *et al.*, Rapid microwave synthesis of CO tolerant reduced graphene oxide-supported platinum electrocatalysts for oxidation of methanol, *J. Phys. Chem. C*, 2010, **114**(45), 19459–19466.
79 J. B. Hou, *et al.*, Electrochemical impedance investigation of proton exchange membrane fuel cells experienced subzero-temperature, *J. Power Sources*, 2007, **171**(2), 610–616.
80 B. Seger and P. V. Kamat, Electrocatalytically active graphene-platinum nanocomposites. Role of 2-D carbon support in PEM fuel cells, *J. Phys. Chem. C*, 2009, **113**(19), 7990–7995.
81 L. F. Dong, *et al.*, Graphene-supported platinum and platinum-ruthenium nanoparticles with high electrocatalytic activity for methanol and ethanol oxidation, *Carbon*, 2010, **48**(3), 781–787.
82 S. Bong, *et al.*, Graphene supported electrocatalysts for methanol oxidation, *Electrochem. Commun.*, 2010, **12**(1), 129–131.
83 R. Kou, *et al.*, Enhanced activity and stability of Pt catalysts on functionalized graphene sheets for electrocatalytic oxygen reduction, *Electrochem. Commun.*, 2009, **11**(5), 954–957.
84 E. Yoo, *et al.*, Enhanced electrocatalytic activity of Pt subnanoclusters on graphene nanosheet surface, *Nano Lett.*, 2009, **9**(6), 2255–2259.
85 T. Yumura, *et al.*, The use of nanometer-sized hydrographene species for support material for fuel cell electrode catalysts: a theoretical proposal, *Phys. Chem. Chem. Phys.*, 2009, **11**(37), 8275–8284.
86 Y. Y. Shao, *et al.*, Highly durable graphene nanoplatelets supported Pt nanocatalysts for oxygen reduction, *J. Power Sources*, 2010, **195**(15), 4600–4605.
87 M. N. Groves, *et al.*, Improving platinum catalyst binding energy to graphene through nitrogen doping, *Chem. Phys. Lett.*, 2009, **481**(4–6), 214–219.
88 R. I. Jafri, *et al.*, Nanostructured Pt dispersed on graphene-multiwalled carbon nanotube hybrid nanomaterials as electrocatalyst for PEMFC, *J. Electrochem. Soc.*, 2010, **157**(6), B874–B879.
89 S. J. Guo, S. J. Dong and E. W. Wang, Three-dimensional Pt-on-Pd bimetallic nanodendrites supported on graphene nanosheet: Facile synthesis and used as an advanced nanoelectrocatalyst for methanol oxidation, *ACS Nano*, 2010, **4**(1), 547–555.
90 L. T. Qu, *et al.*, Nitrogen-doped graphene as efficient metal-free electrocatalyst for oxygen reduction in fuel cells, *ACS Nano*, 2010, **4**(3), 1321–1326.
91 K. P. Gong, *et al.*, Nitrogen-doped carbon nanotube arrays with high electrocatalytic activity for oxygen reduction, *Science*, 2009, **323**(5915), 760–764.
92 Y. Y. Shao, *et al.*, Nitrogen-doped graphene and its electrochemical applications, *J. Mater. Chem.*, 2010, **20**(35), 7491–7496.
93 P. Simon and Y. Gogotsi, Materials for electrochemical capacitors, *Nat. Mater.*, 2008, **7**(11), 845–854.
94 S. R. C. Vivekchand, *et al.*, Graphene-based electrochemical supercapacitors, *J. Chem. Sci.*, 2008, **120**(1), 9–13.
95 J. R. Miller, R. A. Outlaw and B. C. Holloway, Graphene double-layer capacitor with ac line-filtering performance, *Science*, 2010, **329**(5999), 1637–1639.
96 W. Lv, *et al.*, Low-temperature exfoliated graphenes: vacuum-promoted exfoliation and electrochemical energy storage, *ACS Nano*, 2009, **3**(11), 3730–3736.
97 Y. Wang, *et al.*, Supercapacitor devices based on graphene materials, *J. Phys. Chem. C*, 2009, **113**(30), 13103–13107.
98 Y. W. Zhu, *et al.*, Microwave assisted exfoliation and reduction of graphite oxide for ultracapacitors, *Carbon*, 2010, **48**(7), 2118–2122.
99 Y. Y. Shao, *et al.*, Facile and controllable electrochemical reduction of graphene oxide and its applications, *J. Mater. Chem.*, 2010, **20**(4), 743–748.
100 Q. L. Du, *et al.*, Preparation of functionalized graphene sheets by a low-temperature thermal exfoliation approach and their electrochemical supercapacitive behaviors, *Electrochim. Acta*, 2010, **55**(12), 3897–3903.
101 D. W. Wang, *et al.*, Electrochemical interfacial capacitance in multilayer graphene sheets: Dependence on number of stacking layers, *Electrochem. Commun.*, 2009, **11**(9), 1729–1732.
102 X. A. Du, *et al.*, Graphene nanosheets as electrode material for electric double-layer capacitors, *Electrochim. Acta*, 2010, **55**(16), 4812–4819.
103 A. P. Yu, *et al.*, Ultrathin, transparent, and flexible graphene films for supercapacitor application, *Appl. Phys. Lett.*, 2010, **96**(25), 253105.
104 J. Jang, *Conducting polymernanomaterials and their applications*, in *Emissive Materials: Nanomaterials*, Springer-Verlag Berlin, Berlin, 2006, p. 189–259.
105 D. W. Wang, *et al.*, Fabrication of graphene/polyaniline composite paper *via in situ* anodic electropolymerization for high-performance flexible electrode, *ACS Nano*, 2009, **3**(7), 1745–1752.
106 H. L. Wang, *et al.*, Graphene oxide doped polyaniline for supercapacitors, *Electrochem. Commun.*, 2009, **11**(6), 1158–1161.
107 K. Zhang, *et al.*, Graphene/polyaniline nanoriber composites as supercapacitor electrodes, *Chem. Mater.*, 2010, **22**(4), 1392–1401.
108 Q. Wu, *et al.*, Supercapacitors based on flexible graphene/polyaniline nanofiber composite films, *ACS Nano*, 2010, **4**(4), 1963–1970.
109 D. S. Yu and L. M. Dai, Self-assembled graphene/carbon nanotube hybrid films for supercapacitors, *J. Phys. Chem. Lett.*, 2010, **1**(2), 467–470.
110 J. Yan, *et al.*, Preparation of graphene nanosheet/carbon nanotube/polyaniline composite as electrode material for supercapacitors, *J. Power Sources*, 2010, **195**(9), 3041–3045.
111 N. L. Wu, Nanocrystalline oxide supercapacitors, *Mater. Chem. Phys.*, 2002, **75**(1–3), 6–11.
112 F. H. Li, *et al.*, One-step synthesis of graphene/SnO2 nanocomposites and its application in electrochemical supercapacitors, *Nanotechnology*, 2009, **20**(45), 455602.
113 Y. P. Zhang, *et al.*, Capacitive behavior of graphene-ZnO composite film for supercapacitors, *J. Electroanal. Chem.*, 2009, **634**(1), 68–71.
114 T. Lu, *et al.*, Electrochemical behaviors of graphene-ZnO and graphene-SnO2 composite films for supercapacitors, *Electrochim. Acta*, 2010, **55**(13), 4170–4173.
115 M. Toupin, T. Brousse and D. Belanger, Influence of microstucture on the charge storage properties of chemically synthesized manganese dioxide, *Chem. Mater.*, 2002, **14**(9), 3946–3952.
116 S. Chen, *et al.*, Graphene oxide-MnO2 nanocomposites for supercapacitors, *ACS Nano*, 2010, **4**(5), 2822–2830.
117 H. L. Wang, *et al.*, Ni(OH)(2) Nanoplates grown on graphene as advanced electrochemical pseudocapacitor materials, *J. Am. Chem. Soc.*, 2010, **132**(21), 7472–7477.
118 S. Chen, J. W. Zhu and X. Wang, One-step synthesis of graphene-cobalt hydroxide nanocomposites and their electrochemical properties, *J. Phys. Chem. C*, 2010, **114**(27), 11829–11834.
119 F. T. Jiang, *et al.*, Graphene-based carbon nano-fibers grown on thin-sheet sinter-locked Ni-fiber as self-supported electrodes for supercapacitors, *Mater. Lett.*, 2010, **64**(2), 199–202.
120 X. Zhao, *et al.*, Carbon nanosheets as the electrode material in supercapacitors, *J. Power Sources*, 2009, **194**(2), 1208–1212.
121 P. J. Hung, *et al.*, Ideal asymmetric supercapacitors consisting of polyaniline nanofibers and graphene nanosheets with proper complementary potential windows, *Electrochim. Acta*, 2010, **55**(20), 6015–6021.
122 J. M. Tarascon and M. Armand, Issues and challenges facing rechargeable lithium batteries, *Nature*, 2001, **414**(6861), 359–367.
123 A. S. Arico, *et al.*, Nanostructured materials for advanced energy conversion and storage devices, *Nat. Mater.*, 2005, **4**(5), 366–377.
124 M. H. Liang and L. J. Zhi, Graphene-based electrode materials for rechargeable lithium batteries, *J. Mater. Chem.*, 2009, **19**(33), 5871–5878.

125 J. R. Dahn, *et al.*, Mechanisms for lithium insertion in carbonaceous materials, *Science*, 1995, **270**(5236), 590–593.
126 K. Sato, *et al.*, A mechanism of lithium storage in disordered carbons, *Science*, 1994, **264**(5158), 556–558.
127 E. Yoo, *et al.*, Large reversible Li storage of graphene nanosheet families for use in rechargeable lithium ion batteries, *Nano Lett.*, 2008, **8**(8), 2277–2282.
128 C. Y. Wang, *et al.*, Electrochemical properties of graphene paper electrodes used in lithium batteries, *Chem. Mater.*, 2009, **21**(13), 2604–2606.
129 A. Abouimrane, *et al.*, Non-annealed graphene paper as a binder-free anode for lithium-ion batteries, *J. Phys. Chem. C*, 2010, **114**(29), 12800–12804.
130 X. Liu, *et al.*, Composites of molecular-anchored graphene and nanotubes with multitubular structure: A new type of carbon electrode, *ChemSusChem*, 2010, **3**(2), 261–265.
131 D. Y. Pan, *et al.*, Li storage properties of disordered graphene nanosheets, *Chem. Mater.*, 2009, **21**(14), 3136–3142.
132 K. Xu, Electrolytes and interphasial chemistry in Li ion devices, *Energies*, 2010, **3**(1), 135–154.
133 C. Uthaisar and V. Barone, Edge effects on the characteristics of Li diffusion in graphene, *Nano Lett.*, 2010, **10**(8), 2838–2842.
134 T. Takamura, *et al.*, Identification of nano-sized holes by TEM in the graphene layer of graphite and the high rate discharge capability of Li-ion battery anodes, *Electrochim. Acta*, 2007, **53**(3), 1055–1061.
135 P. C. Lian, *et al.*, Large reversible capacity of high quality graphene sheets as an anode material for lithium-ion batteries, *Electrochim. Acta*, 2010, **55**(12), 3909–3914.
136 S. M. Paek, E. Yoo and I. Honma, Enhanced cyclic performance and lithium storage capacity of sno2/graphene nanoporous electrodes with three-dimensionally delaminated flexible structure, *Nano Lett.*, 2009, **9**(1), 72–75.
137 Z. S. Wu, *et al.*, Graphene anchored with Co3O4 nanoparticles as anode of lithium ion batteries with enhanced reversible capacity and cyclic performance, *ACS Nano*, 2010, **4**(6), 3187–3194.
138 S. B. Yang, *et al.*, Fabrication of cobalt and cobalt oxide/graphene composites: towards high-performance anode materials for lithium ion batteries, *ChemSusChem*, 2010, **3**(2), 236–239.
139 D. H. Wang, *et al.*, Self-assembled TiO2-graphene hybrid nanostructures for enhanced Li-ion insertion, *ACS Nano*, 2009, **3**(4), 907–914.
140 G. X. Wang, *et al.*, Sn/graphene nanocomposite with 3D architecture for enhanced reversible lithium storage in lithium ion batteries, *J. Mater. Chem.*, 2009, **19**(44), 8378–8384.
141 S. L. Chou, *et al.*, Enhanced reversible lithium storage in a nanosize silicon/graphene composite, *Electrochem. Commun.*, 2010, **12**(2), 303–306.
142 J. K. Lee, *et al.*, Silicon nanoparticles-graphene paper composites for Li ion battery anodes, *Chem. Commun.*, 2010, **46**(12), 2025–2027.
143 D. W. Choi, *et al.*, Li-ion batteries from LiFePO4 cathode and anatase/graphene composite anode for stationary energy storage, *Electrochem. Commun.*, 2010, **12**(3), 378–381.
144 N. Zhu, *et al.*, Graphene as a conductive additive to enhance the high-rate capabilities of electrospun Li4Ti5O12 for lithium-ion batteries, *Electrochim. Acta*, 2010, **55**(20), 5813–5818.
145 Y. Ding, *et al.*, Preparation of nano-structured LiFePO4/graphene composites by co-precipitation method, *Electrochem. Commun.*, 2010, **12**(1), 10–13.

